Université de Montréal

Fabrication et caractérisation de matrices polymériques structurées pour le génie des tissus articulaires

par Hanauer Nicolas

Axe Formulation et Analyse du Médicament (AFAM), Faculté de Pharmacie

Mémoire présenté en vue de l'obtention du grade de M.Sc en sciences pharmaceutiques option technologie pharmaceutique

Mai 2017

Résumé et mots clés en français

Hypothèse : La fonctionnalisation de blocs hydrogels neutres à l'aide de polyélectrolytes ou de microgels chargés permet leur assemblage contrôlé en milieux aqueux via des interactions électrostatiques

Méthode : Des blocs hydrogels de taille contrôlée ont été photosynthétisés à l'aide d'un support d'injection fabriqué à partir de lames de verre et de photomasques imprimés sur papier transparent. Les formulations se basent sur une structure (hydroxyéthyl)méthacrylate - poly(éthylène glycol diméthacrylate) (HEMA-PEGDMA) interpénétrée soit par du polyéthylèneimine(PEI) chargé positivement soit par de l'acide hyaluronique (HA) chargé négativement. Un autre type de blocs négatifs a été obtenu par le traitement des blocs PEI à l'aide de microgels N-isopropylacrylamide - acide méthacrylique (NIPAM-MAA) chargés négativement. Les propriétés d'assemblage dirigé de deux couples de blocs (PEI-HA et PEI-MG) ont été testées par la mise en contact aléatoire de population de blocs en milieu aqueux. L'effet de la salinité et du pH sur les propriétés d'assemblage ont été étudiés par des tests d'assemblage en milieux salin (NaCl) ou acide/basique.

Résultats : Le support d'injection développé a permis l'obtention de blocs hydrogels de différentes formes et tailles. Différentes fonctionnalisations à base de polyélectrolytes et de microgels ont été testées. Les tests d'assemblage ont résulté en l'obtention d'agrégats de blocs hydrogels liés par des contacts adhésifs spécifiques entre blocs chargés positivement et négativement. Les deux systèmes étudiés présentent cependant des caractéristiques d'assemblage différentes puisque les agrégats PEI-MG sont plus compacts et rigides que les agrégats PEI-HA. En milieu acide (pH=3) et basique (pH=10,5), aucun assemblage n'a pu être

observé. L'augmentation de la salinité s'est accompagnée d'une perte croissante des propriétés d'assemblage. Cet effet délétère du sel est plus marqué pour les systèmes PEI-MG.

Mots-clés : blocs hydrogels, microgels, polyélectrolytes, assemblage dirigé, adhésion

Résumé et mots clés en anglais

Hypothesis: Functionalization of neutral hydrogel blocks with polyelectrolytes and charged microgels allow their directed assembly in aqueous medium via electrostatic interactions

Methods: Hydrogel blocks of controlled size were photosynthesized thank to an injection support composed of glass slides and photomasks imprinted on transparent sheet. Formulations are based on an HEMA-PEGDMA structure interpenetrated either with positively charged PEI or with negatively charged HA. Another type of negative block was obtained by treating PEI blocks with NIPAM-MAA negatively charged microgels. The assembling properties of two block couples (PEI-HA and PEI-MG) were tested by randomly putting in contact block population in water. Effects of salinity and pH on assembling properties were studied with assembling tests in saline (NaCl) or acidic/basic media.

Results: The injection support developed allowed obtaining hydrogel blocks with different shapes and sizes. Various formulations based on polyélectrolytes and microgels were tested. The assembling tests resulted in aggregates formation of hydrogel blocks linked together by specific adhesive contacts between positively and negatively charged blocks. The two systems studied nevertheless present differences in their assembling characteristics: PEI-MG aggregates are indeed more compact and rigid than the PEI-HA aggregates. In acidic (pH=3) and basic (pH=10,5) media, no assembling was observed. The augmentation in salinity resulted in an increasing loss of assembling properties. This deleterious effect was more important for PEI-MG systems.

Key words: hydrogel block, microgels, polyelectrolytes, directed assembly, adhesion

Remerciements

Je tiens à remercier l'ensemble de l'équipe de l'axe Formulation et Analyse du Médicament, dite du 4ème étage, et plus particulièrement aux membres du Labo Banquy.

Table des matières

Liste des tableaux

Liste des figures

Figure 3-5: Effect of salt concentration on the directed assembly of A) PEI/HA and PEI/MG systems B) PEI/MG system in presence of microgels NIPAM-MAA20% at different concentrations. Lines are guides for the eye.
Figure 3-6: Effect of pH on the directed assembly of PEI/HA and PEI/MG systems
Figure 3-7: Models of supposed interactions at hydrogel blocks surfaces during adhesive contacts, A: steric entanglement guided by electrostatic cues between HA and PEI polyelectrolytes chains, B: bridging between PEI chains and NIPAM-MAA microgels without any entanglements involved.

Liste des abréviations

HA: Acide hyaluronique

HEMA: (Hydroxyéthyl)méthacrylate

MAA: Acide méthacrylique

MG: Microgels

NIPAM: N-isopropylacrylamide

PDMS: Polydiméthylsiloxane

PEGDMA: Poly(éthylène glycol diméthacrylate)

PEI: Polyéthylèneimine

Chapitre 1 : Introduction

1-1: Médecine régénérative et ingénierie tissulaire

La médecine régénérative est un domaine émergent des sciences pharmaceutiques et médicales s'intéressant à l'élaboration de traitements basés sur la création de tissus vivants fonctionnels dans le but de soigner ou revitaliser des tissus ou organes endommagés [1,2]. La croissance de tels tissus réparateurs peut être menée *ex-vivo* suivie d'une implantation [3] ou directement *in-vivo*[4-6]. Le développement de telles solutions médicales se base ainsi sur la compréhension, apportée par l'ingénierie tissulaire, de l'influence des facteurs biochimiques (composition du milieu, facteurs de croissance, enzymes…) et physiques (contraintes mécaniques, porosité) sur la différenciation et la prolifération des cellules composant un tissu sain [7-9]. Sans contrôle sur leur croissance, les néo-tissus obtenus ne présentent pas la même organisation structurelle qu'un tissu sain et ne possèdent pas des propriétés biologiques et mécaniques équivalentes. La reproduction spatio-temporelle de contraintes s'approchant du microenvironnement naturel sur des populations cellulaires est donc au cœur des traitements régénératifs [10,11].

1-2 : Échafaudages hydrogels

En réponse à ce problème, l'utilisation de matrices biocompatibles permettant un meilleur contrôle de la croissance cellulaire s'est développée [12]. Ces matrices prennent la forme d'échafaudages polymériques composés d'hydrogels et/ou de fibres polymériques. Le contrôle sur leur structure et leur composition permet de définir l'environnement physique et biochimique des cellules transportées afin d'obtenir un certain contrôle sur leur croissance. Les hydrogels sont de parfaits matériaux pour la réalisation de telles matrices puisqu'ils sont composés d'une part d'une structure polymérique aux propriétés hautement modulables tant

au niveau physique (gonflement, rigidité, porosité…) que chimiques (fonctionnalisations, sensibilité aux conditions environnantes…) et d'autre part d'une phase liquide «immobilisée » permettant l'embarquement de différents composés actifs (espèces chimiques, facteurs de croissance, cellules) [13,14].

Si l'utilisation de tels dispositifs a permis le développement de solutions d'ingénierie tissulaire 2Det 3D pour de nombreux tissus (peau [15,16], cartilage [17,18], os [19]..), une emphase est mise de nos jours sur l'incorporation d'un facteur temporel (relargages rapides ou progressifs, simultanées ou consécutifs de composés actifs, modification des propriétés physiques avec la croissance cellulaire) pour le développement de solutions dites 4D approchant plus l'évolution des conditions environnant la croissance d'un tissu sain. L'article présenté ci-après est une revue de la littérature scientifique sur les dernières avancées dans la livraison 2D, 3D et 4D de composés actifs en médecine régénérative et en ingénierie tissulaire. La 4D correspondant aux 3 dimensions spatiales avec un contrôle temporel. Il a été écrit en collaboration avec Pierre-Luc Latreille, Shaker Alsharif et Xavier Banquy et a été publié en 2015 dans le Volume 21 Numéro 12 de la revue *Current Pharmaceutical Design*.

Article 1: **2D, 3D and 4D Active Compound Delivery in Tissue Engineering and Regenerative Medicine**

Nicolas Hanauer[1], Pierre Luc Latreille[1], Shaker Alsharif[1, 2]and Xavier Banquy[1]

[1] *Canada Research Chair in Bio-inspired Materials and Interfaces, Faculty of Pharmacy, Université de Montréal C.P. 6128, Succursale Centre Ville, Montréal, QC H3C 3J7, Canada*

[2] *Pharmaceutical Chemistry Department, Faculty of Pharmacy, Umm Al-Qura University Al Taif Road, Makkah 24382, Saudi Arabia*

Rôle des auteurs

Shaker Alsharif a effectué les recherches et rédigé la partie sur l'ingénierie tissulaire 2D, Pierre-Luc Latreille sur les échafaudages fibreux et moi-même sur les échafaudages hydrogel. Les recherches et la rédaction ont été effectuées sous la supervision du Pr. Banquy.

Résumé en français

Les avancées récentes dans les domaines de l'ingénierie tissulaire et de la médecine régénérative ont montré que le contrôle du microenvironnement des cellules durant leur croissance est un facteur dé dans le développement de systèmes thérapeutiques efficaces. Pour atteindre un tel contrôle, les chercheurs ont d'abord proposé l'utilisation d'échafaudages polymériques capables de supporter la croissance cellulaire et, dans une certaine mesure, favoriser l'organisation cellulaire et la structure tissulaire. De nos jours, avec la disponibilité de nombreuses lignées de cellules souches, cette approche semble plutôt limitée puisqu'elle n'offre pas un contrôle précis du microenvironnement cellulaire dans le temps et l'espace (4D). Les chercheurs concentrent ainsi leurs efforts sur le développement de stratégies incluant un système de livraison de composés actifs dans le but d'ajouter une dimension aux échafaudages 3D. Cette revue se concentrera sur des concepts et applications récents de techniques 2D et 3D qui ont été utilisés pour contrôler le chargement et le relargage de composés actifs pour

promouvoir la différentiation et la prolifération cellulaire à l'intérieur ou à l'extérieur d'un échafaudage. Nous présenterons les avancées récentes dans le design d'échafaudages polymériques 2D et les différentes techniques utilisées pour le dépôt contrôlé de signaux moléculaires et de cellules. Nous continuerons en présentant les avancées récentes effectuées dans le design d'échafaudages 3D basés sur des hydrogels ou des fibres polymères. Nous finirons en présentant certaines des pistes de recherche encore à explorer.

Abstract

Recent advances in tissue engineering and regenerative medicine have shown that controlling cells micro-environment during growth is a key element to the development of successful therapeutic system. To achieve such control, researchers have first proposed the use of polymeric scaffolds that were able to support cellular growth and, to a certain extent, favor cell organization and tissue structure. With nowadays availability of a large pool of stem cell lines, such approach has appeared to be rather limited since it does not offer the fine control of the cell micro-environment in space and time (4D). Therefore, researchers are currently focusing their efforts in developing strategies that include active compound delivery systems in order to add a fourth dimension to the design of 3D scaffolds. This review will focus on recent concepts and applications of 2D and 3D techniques that have been used to control the load and release of active compounds used to promote cell differentiation and proliferation in or out of a scaffold. We will first present recent advances in the design of 2D polymeric scaffolds and the different techniques that have been used to deposit molecular cues and cells in a controlled fashion. We will continue by presenting the recent advances made in the design of 3D scaffolds based on hydrogels as well as polymeric fibers and we will finish by presenting some of the research avenues that are still to be explored.

Keywords: niche engineering, controlled release, scaffolding, hydrogel, fiber

Introduction

Driven by the increasing demand of organ transplantation, tissue engineering and more recently regenerative medicine have developed numerous strategies to grow such organs *in vivo* or *ex vivo*. After more than two decades of intense research, it is clear that organ engineering requires the use of a scaffold that serves as a synthetic extracellular matrix (ECM) to support and organize cell growth [1-4]. With the increasing number of available biomaterials that possess all the desirable properties required for tissue engineering as well as the constantly widening spectrum of manufacturing techniques to generate complex and finely tuned structures, researchers have been able to develop a tremendous variety of materials and scaffolds designed for specific tissues and applications [5-8]. Within the last few years, the use of stem cells in regenerative medicine and tissue engineering has become predominant [9-13]. Building a suitable micro-environment for their differentiation and proliferation is a challenging task. The rational design of such micro environment must involve a combination of many different expertises such as material micro-engineering, biological engineering and more recently pharmaceutical technology. The requirement of such diverse set of expertise has been driven by the intrinsic behavior of stem cells in their environment [14, 15]. Stem cells are present in many different places in any mammalian organism. They are inherently sensitive to many biophysical as well as biochemical stimuli generated from their direct surroundings [16]. Their differentiation and proliferation is not only dictated by very specific molecules such as growth factors but also by the concentration of such factors and their spatiotemporal distribution in the surroundings [17, 18]. It is believed that these spatiotemporal distributions (also called niche) of key factors are paramount elements determining cell recruitment, migration, proliferation,

protein production and finally organ architecture [19, 20]. Artificially reproducing such complex dynamic environment is the main goal of nowadays tissue engineering research and the main focus of this review article.

Early studies in tissue engineering predominantly used 2D polymeric scaffolds functionalized with adhesives molecules in order to mimic the interactions between cells and the ECM [21, 22]. In parallel, 2D devices such as patches, micro-electro-mechanical-systems or microchips were already reported for the controlled delivery of actives compounds (AC) [23-25]. It is only recently that these two worlds have collided and nurtured each other beneficially. To better mimic biological tissues, the transition from 2D to 3D scaffolds has become a necessary step. Interestingly, the tremendous large body of AC delivery systems using 3D devices such as particles or macromolecules have not been fully explored in tissue engineering. This provides an excellent opportunity for development and promising future discoveries.

Part I: 2D Tissue Engineering

A. Distribution control of molecular cues in 2D

It is well known that most of human body organs and tissues have a 3D structure while some other important body tissues such as blood and lymphatic vessels have a 2D structure. Therefore, engineering of tissues in 2D has proven to be of importance. For this purpose, different technologies in the realm of AC release and cell delivery have emerged in the past few years which we discuss here the most relevant ones (see figure 1).

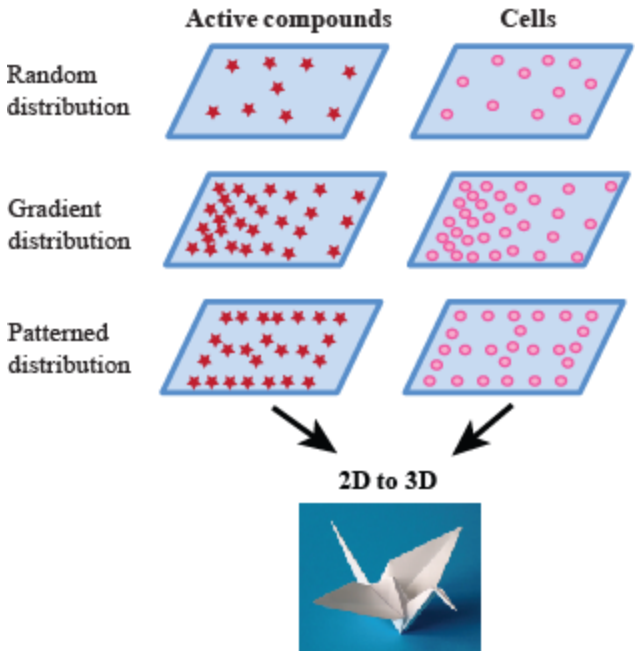

Figure 1-1: AC and cells deposition processes in 2D.

1. Gradient technology

Tissue engineering and regenerative medicine deal directly with ECM, which carries various macromolecules or proteins such as growth factors and chemokines. Their physiological functions such as wound healing and morphogenesis are majorly regulated by molecular concentration gradient phenomena. Many studies related to cellular processes such as *in vitro* migration, signal transmission, cellular proliferation, viability had shown the significance of using gradient materials in tissue engineering [26, 27].

Developing molecular gradients in a material can be extremely challenging especially when it comes to fine controlling. Ostrovidov*et al.*[28] have developed a microfluidic device acting as concentration gradient generator. The device made from micro-engineered poly(ethylene glycol) diacrylate (PEGDA) hydrogel contains concentration gradient of okadaic acid as a model drug released by diffusion. The authors showed that the drug gradient was able to modulate the viability of MC3T3 cells.

Controlling the distribution of AC is not the only benefit of using gradient technology. The mechanical properties of a cell substrate can be controlled as well. *In vitro* techniques based on photolithography [29] or on polymerization of adjoining solutions with variable concentrations [30] in order to obtain crosslinking density gradients have shown that it is possible to achieve good control over the elastic properties of a substrate in 2D.

In a recent study, Tse *et al.*[31] have discussed whether undifferentiated mesenchymal stem cells (MSCs) can experience durotaxis in the absence of any pathological stimulation under exposure to a physiological stiffness gradient. The authors created crosslinking gradient in polyacrylamide hydrogels using radial greyscale pattern with a photomask. In addition, type-I collagen was added to the gradient hydrogel to allow MSCs attachment. Results evidenced that MSCs were subjected to durotaxis on substrates with stiffness gradient values within physiological range and initiated differentiation at the stiffest regions instead of remaining in stationary position as had been hypothesised.

2. Patterning technology

The ability to spatially deposit and control the release of AC of variable size, including drugs and growth factors from patterned biomaterials is crucial to the development of bioactive surfaces for regenerative medicine. One of the scalable methods in patterning such surfaces is lithography. Stern *et al.*[32] have used patterned electropolymerized polypyrroles surfaces to attach and release AC such as ovalbumin and interleukin-2 respectively. These proteins act as vaccine components for binding to dendritic cells that process the antigen and present it to T-cell surface. The patterning was obtained by deposing photoresistant masks on the conductive substrate where electropolymerization of the dissolved monomers containing the AC took place.

The authors showed that surface patterning offered a very high control of the spatial distribution of the AC while their release rate was electrically controlled.

Recent advancement in nanopaterning opens the opportunity to combine colloidal lithography and surface-initiated atom-transfer radical polymerization to finely control molecular cues distribution such as cell adhesive proteins. Li *et al.*[33] used hierarchical polymer brush nanopatterns to graft fibronectin on a planar substrate. As a result, fibronectin was covalently immobilized and showed biological activity without denaturation. Furthermore, MC3T3-E1 mice osteoblasts had cohered to fibronectin patterns immediately and displayed uniformity along the stripes, which suggest that these protein patterns are excellent candidates for cell patterning.

Thissen*et al.*[34] have recently described a method based on surface patterning to control the growth of bovine corneal epithelial tissue on surfaces by creating protein adsorbing and non-adsorbing sites via cell-collagen-I interactions. This manipulation was accomplished by applying a thin layer of acetaldehyde polymer coating (adhesive site for subsequent collagen I deposition) and poly(ethylene oxide) PEO (non-adhesive site) on the substrate.

Common lithographic patterning techniques require either UV exposure or jarring solvents, which are not suitable for most biomolecules. A new patterning technique that does not damage biomolecules was recently reported [35]. The process uses hydrofluoroether solvents which solubilise fluorinated UV resistant materials used to pattern AC through imprint lithography. Such process has been applied to protein and DNA patterning without damaging the AC.

Alternatively, inkjet printing has been used to create spatial patterns of fibroblast growth factor-2 (FGF-2) on fibrin films for studying preosteoblastic cells response *in vitro* [36]. The authors showed that under cell culture conditions for over one week, printed patterns as well as FGF-2 remained persistent and active.

Most of the previously described reports carry great potentials and opportunities for future development regarding tissue engineering. However, it has not been found yet advanced studies involving such methods upon major *in vivo* applications in regenerative medicine.

B. Cell patterning and co-culture

Spatial control of living cells distribution has attracted great attention due to its broad potential applications in regenerative medicine. The development of microfabrication technology in the past decade has largely enriched cell patterning methods by introducing precise surface engineering, in which spatial patterning of cells is confined by regulating surface chemistry. Cells are often patterned on a planar surface, which can be further controlled to prepare a 3D bioactive structure or scaffold.

Inkjet printing method was reported as an advantageous technique for human fibroblast cells patterning. Using this method Saunders *et al*. [37] were able to create cells patterns on agarose gel without damaging the cells.

In order to modify surface chemistry and to improve cell patterning, Chien *et al.*[38] have combined microcontact-printing method with mussel inspired surface chemistry. Controlled imprints of polydopamine (PDA)/poly ethylene imine (PEI) were fabricated using poly(dimethylsiloxane) (PDMS) stamps. These imprints were used to control cell adhesion using the high binding affinity of PDA enhanced by deposition of PEI. *In vitro* tests conducted with co-cultured hepatocytes and neural cells lead to spatially controlled distribution of cells. This technique could be used to favor cells adhesion at specific sites by recover them of cell adhesion promoting imprints.

In another study Tanaka *et al.*[39] discussed how to manage the PDMS stamping force and the importance of stamp stiffness to improve cell patterning. The authors reported a method to

improve printing precision by controlling the stamp stiffness via microscope observation of stamp deformation due to the applied force. The proposed micro printing method gave a high printing quality with 2.5% error of micro stamping area and was tested by patterning GFP-HUVEC (GFP Expressing Human Umbilical Vein Endothelial Cells) and NIH/3T3 co culture on fibronectin covered substrates (see figure 2)

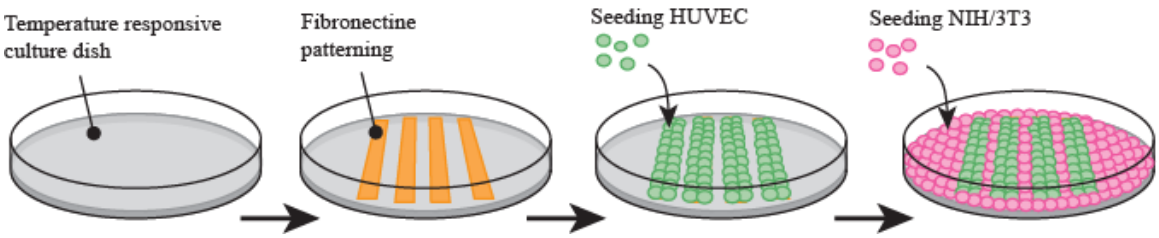

Figure 1-2: Two-cell patterned co-culture, adapted from [39].

C. 3D constructs based on 2D assemblies

In the area of 3D microfabrication, a recent novel strategy based on 2D scaffold folding, which enables production of 3D microstructure simply by folding 2D sheets was recently reported [40]. Origami folding and polyhedral capsule rolls are two examples using such strategy [41].

Bioartificial endocrine pancreas (BAEP) was created by encapsulating pancreatic B-cells for diabetes treatment purposes [42]. This BAEP was found more advantageous over gel encapsulation method in terms of mass transfer efficiency of AC due to its unique architectural design and geometry. The BAEP fabrication was based on folded polyhedral capsules wrapped up within an alginate sheet (see figure 3). Consequently, insulin release was confirmed suggesting that this approach could be convenient for regenerative medicine.

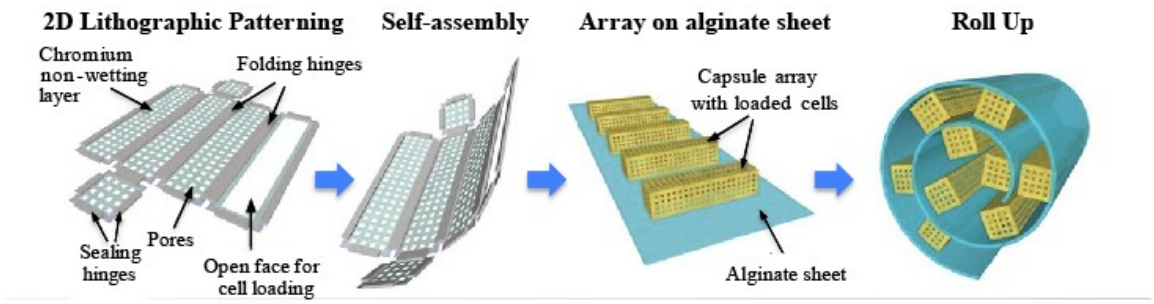

Figure 1-3: BAEP fabrication, adapted from [42].

This emerging technology is extremely promising due to its potential scalability, its versatility in terms of structures and materials that can be used. Such approach though, requires very specific expertises and equipment which limits its exploration and use at the present time. Instead, other approaches based on readily available materials such as hydrogels have attracted much more attention and will be described in the next section.

Part II: Hydrogel scaffolds

Techniques of 3D hydrogels scaffolding have been developed for two major regenerative medicine related purposes: cell viability, proliferation and differentiation as well as AC delivery [43]. This was commonly achieved by the incorporation of AC and/or cells inside the hydrogel matrix via different techniques leading to various architectures that can be used for diverse applications (see figure 4).

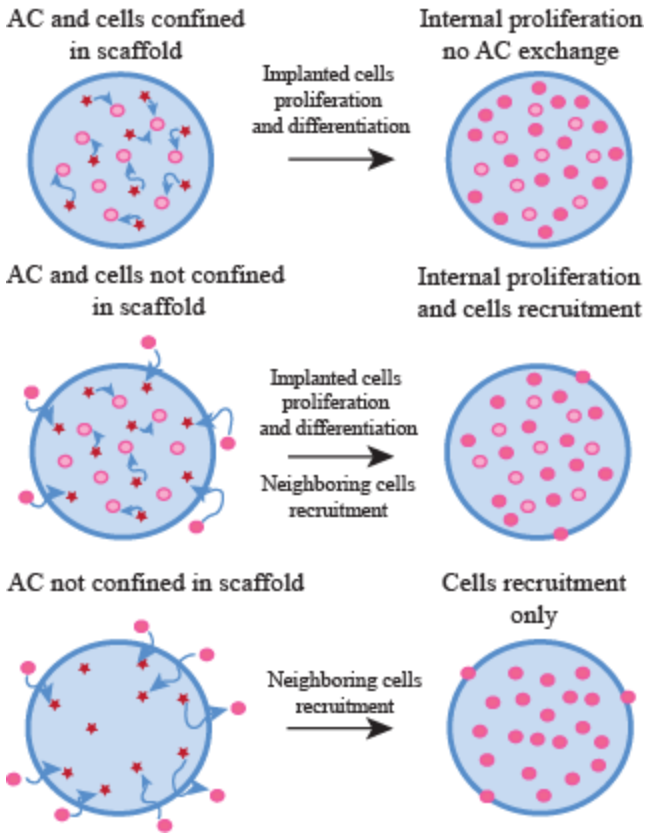

Figure 1-4: Strategies for tissue growth based on AC delivery.

A. Effect of active compounds loading and release

Incorporating an AC such as a growth factor, a drug or genetic material into a polymeric scaffold can be achieved by embedding this compound inside the scaffold using chemical or physical bounding [44]. Control over such bindings and loading mechanics is a key parameter to achieve simultaneous or sequential controlled release of multiple AC [45].

Incorporation of an AC into a hydrogel matrix usually results in a fast release of the AC, at least during the initial period of the release (see figure 5). Such effect, known as initial burst effect is problematic for tissue engineering applications where long lasting delivery is often desirable. Tang *et al.*[46] have controlled the burst effect by embedding N-(2-hydroxyl) propyl-3-trimethyl ammonium chitosan chloride (HTCC) – carboxymethyl chitosan (CM) nanoparticles into

chitosan/poly(vinyl alcohol) hydrogel by adding them prior to gelation. Propranolol, as positively charged model drug, diclofenac sodium, as negatively charged model drug, and nanoparticles were added prior to gelation. The authors obtained nanoparticles with different charges by varying the ratio between HTCC and CM. The interaction between the drug and the nanoparticles was shown to have a direct effect on the release. The release of the positively charged drug was found to be much slower in negatively charged hydrogel than in neutral hydrogel and *vice versa*.

The controlled release of growth factors is crucial in regenerative medicine due to their roles as biological cues for cell fates. Pakulska *et al.*[47] have prepared chondroitinase ABC (ChABC), a promising therapeutic agent for spinal cord injury to a methylcellulose (MC) hydrogel by grafting a small protein domain (Src homology 3: SH3) on the AC and a binding peptide (weak or strong) on the hydrogel. The release rate of the AC was then tuned either by varying the SH3-protein/SH3-peptide pair binding strength or ratio. Even if the release process was disturbed by the thermal instability of ChABC at 37°C, the authors were able to observe a tunable release: 90% of release was obtained after 3 days for an unmodified MC hydrogel, while it decreased to 20% in 7 days with the strong ChABC-SH3 binder and to 50% and 10% in 7 days with a weaker binder at respectively 100 and 300-fold molar excess of SH3 peptide to ChABC.

AC release can be triggered by cell activity as well. Song *et al.*[48] have studied the effect of combining two AC (stromal derived factor 1: SDF-1 and angiogenic peptides: Ac-SDKP) in an acrylated hyaluronic acid hydrogel on a chronic myocardial infarction rat model. The authors loaded SDF-1 directly within the hydrogel and Ac-SDKP was bound to the polymer scaffold via thiol-acrylate reaction. The release of SDF-1 and Ac-SDKP was triggered by the action of matrix metalloproteinase (MMP) secreted by the surrounding cells or via hydrogel degradation. By providing an injectable 3D micro-environment to attract mesenchymal stem cells followed by

growth factor release, this approach was found to promote stable vessels growth, and decreased fibrosis, which in turn leads to the recovery of heart function. Even if the mechanism of regeneration by SDF-1 and Ac-SDKP is still unclear, this study showed the strong positive synergistic effect of the two compounds.

These recent examples show that AC controlled loading and release in hydrogel scaffold play a crucial role for the development of therapeutic implants. By tuning the hydrogel scaffold properties and especially the AC-matrix bounding, multiple and sequential releases of ACs can be envisaged.

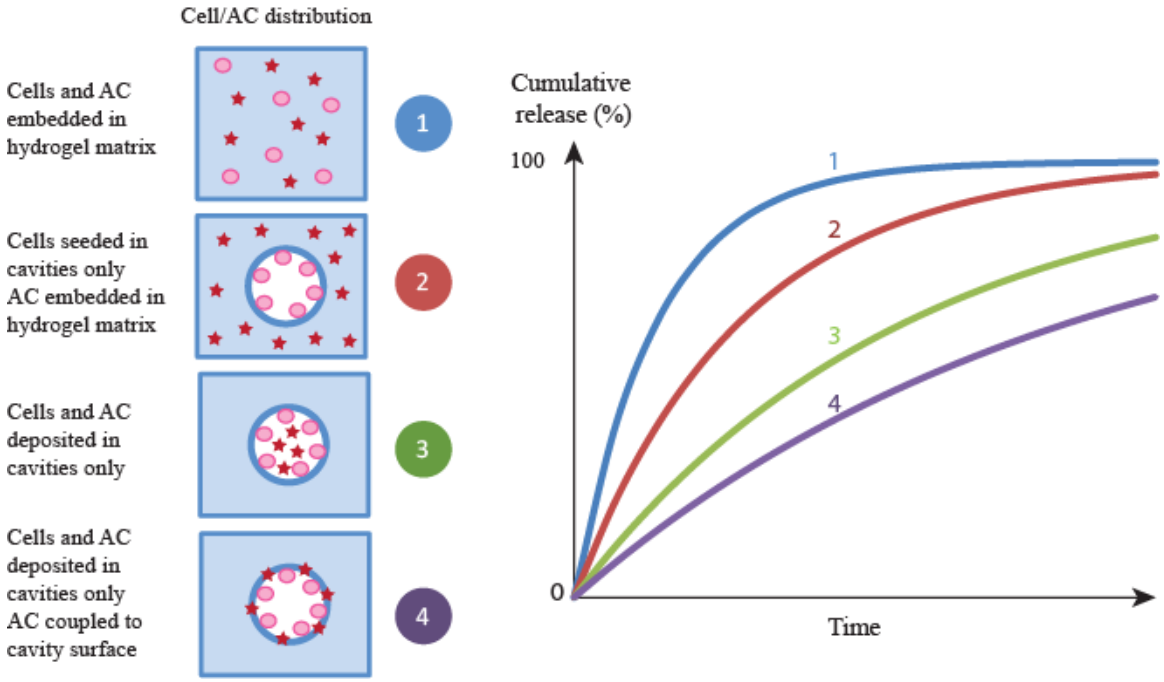

Figure 1-5: Expected cumulative release of different cells/ACs distributions in hydrogel scaffolds.

B. Effect of cells loading and culture

Due to their internal structure that can be tuned to mimic the ECM, hydrogels were firstly used for cell immobilization [49]. With the development of tissue engineering and progress in hydrogel scaffolding, these materials are now able to promote cells growth, differentiation and

organization [50, 51]. Such properties can be achieved via incorporation of cells into structured 3D hydrogel scaffolds in multiple ways depending on what the final goal or application is.

Cell embedment in the hydrogel can be achieved by directly inserting the cells during the gelation process. Wright *et al.*[52] studied human corneal epithelial cells viability in a calcium alginate-hydroxyethyl cellulose hydrogel. After mixing the cells with the hydrogel solution, cells were found to survive the gelation process, and were viable up to 7 days in ambient and chilled conditions, which makes this hydrogel potentially useful for cells transport and storage purposes.

Such technique can also be used to highlight the role of the hydrogel composition on loaded cells fate. Li *et al*[53] used fluorinated methacrylamide chitosan hydrogels for neural stem cell differentiation. Neural cells were added with scaffold components prior to photopolymerization. The authors studied the proliferation and differentiation of neural cells in fluorinated methacrylamide chitosan hydrogels which had the ability to uptake oxygen from the environment or from supplemental oxygen. Fluorine moieties in the hydrogel were found to modulate oxygen uptake and release which resulted in improved cell proliferation and differentiation.

Introducing the receptor sites in the hydrogel is an easy way to increase the amount of introduced cells and to achieve a better control over their near environment. Halstenberg *et al.*[54] created an artificial protein with matrix degradation capacity containing two cell binding sites (RGD integrin-binding and heparin binding site), matrix degradation sites (two plasmin degradation sites) and an acrylate moiety. The authors used this protein in conjunction with poly(ethylene glycol) diacrylate to form a hydrogel. Human fibroblasts-fibrin clusters were embedded via cell solution deposition on the hybrid hydrogel. These clusters were used to assess cell attachment on 3D binding sites, proliferation for at least 7-9 days *in vitro* and cell

induced matrix degradation. Using the artificial protein resulted in an improved cellular penetration in the hydrogel due to the combination of cellular outgrowth and triggered matrix degradation.

Incorporation of niches inside the hydrogel matrix prior to cell embedment was found to have positive effect on cells development. Hwang *et al.*[55] used gelatin beads (150-300µm) included in a cell laden alginate hydrogel, which after dissolution and washing left occlusions of controlled size. Use of such scaffolds in tissue engineering was tested using hepatocarcinoma cells (HepG2). The cells were positioned inside the cavities and significantly enhanced cell proliferation was observed compared to non porous scaffold, due to better mass transfer of nutrients, oxygen and waste removal through the hydrogel.

C. Active carriers for tissue regeneration

Cell fate in a tissue depends on two main factors: mechanical stress and cell-ECM biochemistry. Chemical interactions between cells and AC are based on 3D-signaling which is a result of AC spatiotemporal availability and cells motility. Active carriers for tissue regeneration combine cells encapsulation and triggered AC release to promote timed-control cell growth.

Du *et al.*[56] obtained chitosan hydrogel exhibiting an interconnected network of cavities using 10 µm $CaCO_3$micropartides encapsulation followed by gas foaming. After freeze-drying treatment of the hydrogel, the authors obtained a hierarchical porous structure later treated by layer-by-layer molecular deposition of oppositely charged chondroitin sulfate (CS) and chitosan to mimic the ECM. The hydrogel cavities were then loaded on their surface with fibroblast growth factor (FGF) via CS binding and then with human lung fibroblast cells. The authors showed that the architecture of the interconnected network of cavities did not have any significant effect on FGF cumulative release but improved FGF loading resulting in a higher

amount of FGF reaching encapsulated cells (see figure 6). The authors showed that combining the hierarchical porous structure of the chitosan hydrogel with the controlled loading and release of the growth factor via CS binding of FGF had a positive effect on human lung fibroblast growth.

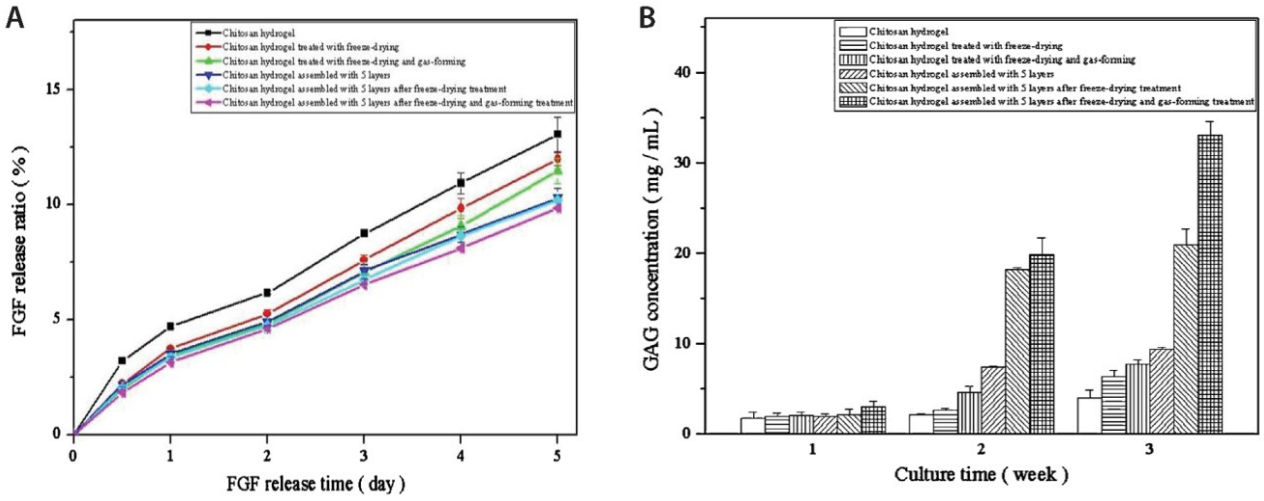

Figure 1-6: Release curve of FGF (**a**), FGF loaded (**b**) and variation of GAG concentration (**c**) in different chitosan hydrogel treated by freeze drying and/or by gas foaming prior to layer-by-layer assembling of chondroitin sulfate and chitosan. Adapted from [56].

In another study, the same authors [57] used two growth factors that could be released successively. They incorporated two growth factors, native TGF-β and bFGF modified to specifically bind to collagen in a CS/collagen hydrogel. Such modification allowed the growth factor to be loaded in the scaffold to a much higher content and to be released much slower than TGF-β. These successive releases were used by the authors to induce differentiation of hMSCs into chondrocytes (see figure 7).

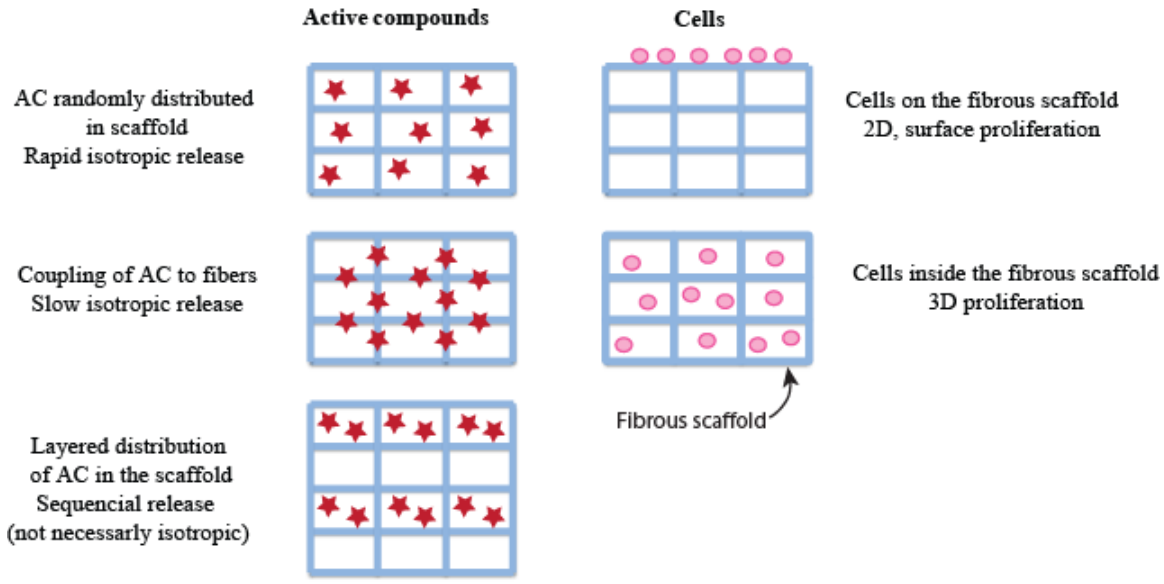

Figure 1-7: Representation of possible uses of fibrous scaffolds in drug encapsulation and in cell encapsulation.

Hydrogel scaffolds have been tested *invivo* as well. Using direct loading of two growth factors (VEGF: vascular endothelial growth factor and IGF-1) in an alginate hydrogel precursors mix prior to gelation and followed by freeze drying to create a niche for myoblast encapsulation lead to a scaffold able to promote musde regeneration. Borselli*et al.*[58] tested this hydrogel in the context of a severe injury to mice skeletal muscle tissue. A synergistic effect between VEGF and SDF-1was demonstrated on musde growth in comparison to implantation of blank alginate scaffold or single growth factor loaded hydrogel. It was also shown that cell seeding in the hydrogel allows even better musde regeneration. Even if the impact of such scaffold on the muscle size and weight was not always significant, it allowed an improved fiber growth and higher blood vessel density leading to normal tissue perfusion levels.

It is possible also to pattern the hydrogel containing growth factors and cells before implantation in order to better mimic *in vivo* tissue organization. Chen *et al.* [59] have combined two genes (TGF-B1 and BMP-2) activated chitosan/gelatin scaffolds (freeze dried for

mesenchymal stem cell loading) to create a bilayered hydrogel for articular cartilage and subchondral bone simultaneous regeneration. Once both scaffold were loaded with mesenchymal stem cells and have supported cells differentiation (chondrogenic and osteogenic respectively), they were glued together via fibrin glue. The bilayered materiel was tested on a rabbit knee defect and was found to perfectly support articular cartilage and subchondral regenerations, leading to complete repair.

The strategies described so far involve controlled but passive release of the AC. This is, in principle, not efficient to maximize contact of the AC with the surrounding cells. To overcome this problem Yang *et al.*[59] developed an active PEG scaffold able to release locally synthetic glucocorticoid Dexamethasone (DEX) only in presence of a neighboring cell. The authors conjugated DEX to the scaffold using a peptidic linker. The linker was degraded by production of matrix metalloproteinase from the proliferating hMSCs. This resulted in a localized stimulation of alkaline phosphatase (ALP) and calcium deposition for over 21 days whereas no elevated cellular responses were observed in co-cultured hMSCs surrounding the gel, suggesting possible applications in bone regenerative medicine.

With their highly tunable internal structure, hydrogels are the main material used for scaffolding. Such scaffolds have various applications for regenerative medicine going from storage to multiple controlled releases of AC and/or cells. Even if some hydrogel scaffolding techniques are already commercially available, the innovations discussed above present promising future as therapeutic treatments. However hydrogel scaffolding is not the only solution for 4D AC delivery, other materials are gaining interest, such as fibrous scaffolding.

Part III: Fibrous scaffolds

Fibrous scaffolds represent a popular substrate for tissue engineering. Their fibrous nature mimics biological tissues matrices at a microscopic scale compared to plain materials such as hydrogels. Many strategies were developed and characterized in an objective of delivering AC and cells to animals (see figure 7). As mentioned, those concepts focused on the control of AC release from promising fibrous scaffolds have emerged and are summarized in the next section.

A. Controlled release of AC from fibrous scaffolds

Many different strategies exist to incorporate an AC into a fibrous material [60-62]. Most of them face a common problem of short release time which is problematic from a tissue engineering perspective. To tackle this problem, a first approach consists in using structured fibers. Novajra *et al.* [63] have recently developed a biodegradable scaffold based on hollow fibers of biodegradable glass for the long term release of neurotropic factors. Fibers were filled with genipin crosslinked agar/gelatin hydrogel in presence of fluorescein isothiocyanate-dextran (FD-20). The authors did not report any correlation of the release rate and the fibers diameter since all of them achieved 100% release of FD-20 after 24h. Also, no significant cytotoxicity of fiber dissolution products was reported on neonatal rat olfactory bulb ensheathing cell line.

Another efficient strategy to develop structured fibers is to use mixture polymers during the electrospinning process. Bonani *et al.*[64] have developed a fibrous scaffold by making use of electrospunnanofibers of poly ε-caprolactone (PCL) and poly(D,L-lactide-*co*-glycolide acid) (PLGA). The authors designed different patterns of fibers of PCL and PLGA by spatially controlling their distribution on both side of the scaffold. Therefore, PLGA (with ending carboxylic group, PLGAac or with ester end group, PLGAes) polymers were loaded with either rhodamine B (RhB), fluorescein or tetra-methyl-rhodamine conjugated bovine serum albumin (AlbF and AlbT) to

perform double-sided release. PLGAac-PCL and PLGAes-PCL releasing RhB (from a uniform gradient of PLGA-PCL polymers) both showed a majorly one-sided release with a burst effect. PLGAes has demonstrated lower side release selectivity. Release of AlbT of PLGAac-PCL with the same gradient showed that 24% of protein was released in 24 hours and 80% was released in 9 days on mainly one side only of the scaffold. After this period, the authors had estimated a constant release rate of AlbT of 1% per week. Moreover, the authors were able to sequentially release both proteins (AlbT and ALbF) by altering the materials distribution in the scaffold (see figure 8). Highest release rate of AlbT occurred at the first day, while AlbF release was delayed until day 5. A similar approach was used to release AlbT and AlbF each one from a different side of the scaffold.

Alternatively, Lee *et al.* [65] successfully immobilized bone-forming peptide-1 BFP-1 on the surface of PLGA fibers coated with PDA and then characterized the differentiation of hMSCs into osteocytes and bone volume increase in mice calvarial defect models. hMSCs culture has shown for BFP-1 immobilized fibers higher cellular differentiation, calcium production and ALP activity than controls (PLGA and PLGA-PDA coated scaffolds). Similar correlations were also observed *in vivo* in the mice calvarial defect models. Immobilization of the growth factor at the surface of the fibrous scaffold significantly increased bone regeneration in animal model by potentially increasing cell differentiation and ALP activities, supported by *in vitro* results.

Fibrous scaffold based on polyester polymers such as PLA, PLGA or PCL are most commonly used without any further modifications [66]. An improvement to this methodology is to build hybrid scaffolds incorporating different components within the fibers designed to perform very specific tasks. In that line of research, Lee *et al.*[67] have incorporated a self-assembled nanofiber gel of heparin-binding peptide amphiphiles (HBPA) and heparin-sulfate (HS) into a porous collagen scaffold. The objective was to increase bone regeneration by mimicking biological BMP-2

signaling. The authors found that the natural affinity of BMP-2 to HBPA/HS complex made it able to modulate its release from the nanofibers gel. Implantation of the hybrid collagen scaffold loaded with low dose of BMP-2 significantly increased bone regeneration compared to controls in a rat model of femoral defect. These results clearly demonstrated that the architecture of the scaffold or its capacity to release AC are not the only crucial factors determining tissue regeneration. Incorporation of key signaling mechanism of the ECM can certainly amplify the regenerative capacity of growth factors as well.

Silk fibers are increasingly used as scaffolds for their biodegradability, biocompatibility and mechanical properties and were found to be very suitable for bone tissue bioengineering [68-70]. Li *et al.*[71] designed a scaffold using electrospun silk fibers, poly(ethylene oxide) and incorporated nanopartides of hydroxyapatite (silk/PEO/nHAP). BMP-2 was incorporated in the scaffold without any specific link and hMSCs were seeded on the surface of the scaffolds. Higher deposition of calcium and presence of bone-specific markers of differentiated hMSCs was observed and presence of nHAP further improved the results compared to controls. A similar scaffold developed by Biman*et al.* [72] utilized silk fibers embedded in polyacrylamide hydrogel. The authors showed, by using different fibers/hydrogel ratios, that the release rate of a model peptide (FITC linked insulin) increased significantly at higher concentration of fibroins in the scaffold.

B. Encapsulation of cells into fibers

Scaffold designed for cell delivery aim to recreate microenvironments with 3D cell-cell interaction of tissues. Promoting such 3D interaction might constitute a major leap for the treatment of a broad spectrum of degenerative diseases. Onoe*et al.*[73] developed a calcium alginate micro-fibrous hydrogel (Ca-alginate) embedding cells and ECM proteins. These fibers

were generated from a double-coaxial microfluidic device with a flow of hydrogel and ECM with cells. Cells were then cultured until a cell fiber had being formed and the Ca-alginate was removed to obtain a cell-ECM fiber. Using a weaving and reeling technique, the authors were able to produce a scaffold with multiple cell fibers. This technology was then tested in diabetic mice model in the attempt to treat mellitus diabetes. The authors injected pepsin-solubilized type I collagen as ECM and fibers made of rat dissociated pancreatic cells and mouse pancreatic beta cells into the subrenal capsular space. After implantation, a significant decrease in blood glucose concentration was found while upon removal, blood glucose levels were readjusted to their initial concentrations, demonstrating efficacy for diabetes treatment. Potentially, this technique is very promising for fibrous scaffolding in regenerative medicine because of its versatility of application along with its customizability of ECM patterning, cell type or cell line.

Similarly, Wan *et al.*[74] fabricated an interesting multi-component hydrogel fibers made from water soluble chitin (WSC) and sodium alginate in a matrix of WSC, galactose and collagen to spatially co-culture differentiated human hepatocytes and endothelial cells. The resulting 3D fibrous scaffold was utilized for encapsulation and culture of differentiated cells and then implanted in mice where 70% of the original liver was removed. Human albumin in mice serum was detected at 2 and 4 weeks after implantation. The addition of structured endothelial cells to human hepatocytes on fibers increased albumin secretion *in vivo*.

Electrospun fibers recently received increased attention as a potential AC and cell encapsulating and delivering scaffold [75-78]. The capacity to guide cell adhesion and simulating native ECM makes this material attractive for various cellular applications. Mirahmadi *et al.*[79] prepared different hybrid scaffolds of chitosan/glycerophosphate (CS/GP) hydrogels by incorporating electrospun silk fibroins. No cytotoxicity was reported on seeded chondrocytes. Silk fibers incorporated in the scaffold increased glycosaminoglycan production after 21 days. This

production was further increased by homogenous dispersions of silk fibers. Scaffolds comprising homogenously dispersed fibers in the hydrogels produced lower collagen II amount compared to a multi layered construct. The authors concluded that the multi-layer construct was the most suitable for collagen and proteoglycan deposit and therefore the most viable option for cartilage tissue engineering.

Using a comparable method, Xiao *et al.*[80] incorporated different concentration of silk fibroins into a gelatin methacrylate (Gel-MA) hydrogel scaffold. NIH-3T3 cells were seeded on the surface of the scaffold. The authors showed that cell spreading was similar for all fiber concentrations tested, including blank Gel-MA hydrogels. Cell number was consequently higher among the lowest fiber concentrations and blank Gel-MA hydrogels. Interestingly, similar results for metabolic activities after 5 days were reported. Scaffolds presenting the lower fibroin concentration (5 $mg.mL^{-1}$) in Gel-Ma hydrogels were displaying the best properties for regenerative medicine application.

C. Promoting regeneration with cells and growth factor delivery in fibrous scaffold

As mentioned previously fiber electrospinning is a process suitable for creating fibers of various materials. The convenience of growth factors loading as well as simultaneous cells incorporation lead Du *et al.*[81] in making use of CS/PCL electrospun nano fibers. By controlling the distribution of CS in the scaffold, either highly concentrated at the surface or homogeneously distributed, the authors were able to tune the distribution and release of VEGF from the scaffold. The release of VEGF was measured and the burst effect from the gradient scaffold was found approximately 42.5% reduced in comparison to uniformly loaded scaffold (see figure 9). After approximately 72 hours, nearly 80% of the total loading was released scaffolds for both. Cytotoxicity assay on human umbilical vein endothelial cells (HUVECs) cultured on fibers was

performed testing 4 preparations: both uniformed and gradient scaffolds with or without immobilized VEGFt. Gradient scaffold with VEGF presented significant increased cell growth compared to the three other scaffolds after 24h, 48h and 72h incubation time, but not after 4h and 12h (see figure 9). Co-culture of HUVECs and vascular smooth musde cells (vSMCs) on the CS/PCL-VEGF gradient scaffold demonstrated that HUVEC were proliferating on the surface of the scaffold to form a monolayer, while vSMCs were growing at the bottom surface, forming a vascular-like structure.

Alternatively, Lee *et al.*[82] combined photolithography and electrospun fibers of PCL/gelatin in a poly(ethylene glycol) (PEG) micropatterned hydrogel. According to the authors, the technique has the potential to release multiple growth factors in a controlled fashion to help stem cells to differentiate. The authors first synthesized PCL-gelatin fibers and then PEG hydrogel was micropatterned on the fibers by photopolymerisation in presence of bone morphogenetic protein-2 (BMP-2) in solution. The resulting composite gel was swollen into basic fibroblast growth factor (bFGF) solution in order to load bFGF on the surface of the exposed fibers. Both loaded growth factors (BMP-2 and bFGF) were released in PBS. The release of bFGF deposited on the fibers was faster with a significant burst during the first days, while BMP-2 entrapped in the hydrogel scaffold exhibited a slower burst extended over 5 days. Both factors showed a slow release rate for 30 days after burst release. The authors demonstrated that hMSCs proliferated only on PCL/gelatin fibers and not on PEG micropatterns. BMP-2 and combination of BMP-2/bFGF significantly increased hMSCs differentiation compared to bFGF and control, suggesting that bFGF had no effect on both parameters. Faster differentiation into osteocytes was also correlated to stronger mineralisation.

Alternating layer of fibers may also be an interesting avenue to achieve a structured material capable of releasing AC and delivering stem cells. Manning *et al.*[83] created a scaffold

alternating 11 layers of electrospun PLGA nanofiber and heparin/fibrin-based delivery system (HBDS). The release profile of platelet-derived growth factor (PDGF) was measured for fibrin and HDBS with and without fibers. PDGF was released faster from fibrin and slower for HDBS and fiber addition was found to have a versatile effect, decreasing the release rate with fibrin and increasing it for HDBS. *In vivo* cell viability tests using adipose stem cells were performed on adult mongrel dogs and shown successful cell delivery and viability after 9 days.

Lee *et al.*[84] have demonstrated that hydroxyapatite mineralized polycaprolactone-gelatin fibers (PCL-gelatin), combined with a fibronectin fusion protein and osteocalcin (OCN), were able to stimulate hMSC functions. A release study of FN-OCN on non-mineralized fibers have shown that release was completed after 3 days, while for mineralized fibers only, 10-15% was released in 10 days, showing a more sustainable release. *In vitro* models, using hMSCs, comparing fibers with and without FN-OCN protein showed that cells were adhering and spreading faster in presence of FN-OCN protein. Further *in vivo* testing in a rat calvarium model showed that mineralized PCL-gelatin fibers with FN-OCN were increasing bone volume and density compared to PCL-gelatin without FN-OCN protein. Moreover, the addition of hMSCs and OCN in the scaffold further increased bone volume, but not density.

Conclusion

As we just described, fine control of AC release from a scaffold can be achieved in many different ways. The most commonly used strategies to date involve either the physical conjugation of AC to the scaffold, the encapsulation of the AC into a drug delivery system embedded into the scaffold or the direct incorporation of the AC into the scaffold. These approaches have shown to be able to modulate, to a certain extent, the release profile of the AC from a few hours to several weeks. Correlation between internal structure and AC release is the

key parameter to use such scaffolds for tissue engineering and regenerative medicine applications. Mimicking internal architecture and AC regulation of native tissue allows controlling cells fate and organization which dictate neo-tissue properties. As we have seen, 2D gradient and patterning technologies have been developed for many years but their transition to 3D and 4D AC release is not yet achieved. Even if 3D printing, currently an important field of experimentations, and folding technique, a more recent explored phenomenon, show interesting properties for scaffold design, their capacity for AC embedment still needs to be improved. Due to their tunable internal structure, hydrogels and fibers have been majorly used for regenerative medicine scaffold systems development. These systems complexity is increasing, resulting in a better control over AC release, but it could also be a drawback over their transition to clinical use. Future development of such systems will have to put emphasis on cells environment via controlled organization and multiple triggered AC release. Nevertheless, besides the large body of work that have been reported, it is quite surprising to notice that only a few systematical studies have tried to quantitatively correlate AC release profile to cell differentiation and proliferation. In fact, the few existing studies, as we showed in this review, are performed *in vitro* and do not focus on such correlations yet. It is also interesting to notice that besides the extremely rich population of drug delivery systems that have been designed and tested *in vivo*, only a handful have been incorporated into an engineered scaffold. Such observation confirms that the control of AC release, in space and time (4D) can still be improved and explored in order to improve existing regenerative therapies.

References

[1] Yang SF, Leong KF, Du ZH, Chua CK. The design of scaffolds for use in tissue engineering. Part 1. Traditional factors. Tissue Eng., 2001; 7: 679-689.

[2] Yang SF, Leong KF, Du ZH, Chua CK. The design of scaffolds for use in tissue engineering. Part II. Rapid prototyping techniques. Tissue Eng., 2002; 8: 1-11.

[3] Langer R, Vacanti JP. Tissue engineering. Science (New York, N.Y.), 1993; 260: 920-6.

[4] Rabanel JM, Banquy X, Zouaoui H, Mokhtar M, Hildgen P. Progress technology in microencapsulation methods for cell therapy. Biotechnol. Prog., 2009; 25: 946-963.

[5] Hutmacher DW, Goh JC, Teoh SH. An introduction to biodegradable materials for tissue engineering applications. Ann. Acad. Med. Singapore, 2001; 30: 183-91.

[6] Kytai Truong N, Jennifer LW. Photopolymerizable hydrogels for tissue engineering applications. Biomaterials, 2002; 23.

[7] Pham QP, Sharma U, Mikos AG. Electrospinning of polymeric nanofibers for tissue engineering applications: a review. Tissue Eng., 2006; 12: 1197-211.

[8] Chen W, Tabata Y, Wah Tong Y. Fabricating tissue engineering scaffolds for simultaneous cell growth and drug delivery. Curr. Pharm. Des., 2010; 16: 2388-2394.

[9] X. W. Spatial Effects of Stem Cell Engagement in 3 D Printing Constructs. Journal of Stem Cells Research, Reviews & Reports, 2014; 1.

[10] Eberli D, Atala A. Tissue engineering using adult stem cells. Methods Enzymol., 2006; 420: 287-302.

[11] Ciapetti G, Granchi D, Baldini N. The combined use of mesenchymal stromal cells and scaffolds for bone repair. Curr. Pharm. Des., 2011; 18: 1796-1820.

[12] Thorrez L, Sampaolesi M. The future of induced pluripotent stem cells for cardiac therapy and drug development. Curr. Pharm. Des., 2011; 17: 3258-70.

[13] Pelled G, Turgeman G, Aslan H, Gazit Z, Gazit D. Mesenchymal stem cells for bone gene therapy and tissue engineering. Curr. Pharm. Des., 2002; 8: 1917-1928.

[14] Bianco P, Robey PG. Stem cells in tissue engineering. Nature, 2001; 414: 118-121.

[15] Caplan AI. Adult mesenchymal stem cells for tissue engineering versus regenerative medicine. J. Cell. Physiol., 2007; 213: 341-347.

[16] Tuan RS, Boland G, Tuli R. Adult mesenchymal stem cells and cell-based tissue engineering. Arthrit. Res. Ther., 2003; 5: 32-45.

[17] Lutolf MP, Hubbell JA. Synthetic biomaterials as instructive extracellular microenvironments for morphogenesis in tissue engineering. Nat. Biotechnol., 2005; 23: 47-55.

[18] Adam C, Mathis R. Tissue engineering: the biophysical background. Phys. Med. Biol., 2001; 46: R47.

[19] Place ES, Evans ND, Stevens MM. Complexity in biomaterials for tissue engineering. Nat. Mater., 2009; 8: 457-470.

[20] Rezwan K, Chen QZ, Blaker JJ, Boccaccini AR. Biodegradable and bioactive porous polymer/inorganic composite scaffolds for bone tissue engineering. Biomaterials, 2006; 27: 3413-3431.

[21] Nikolovski J, Mooney DJ. Smooth muscle cell adhesion to tissue engineering scaffolds. Biomaterials, 2000; 21: 2025-32.

[22] Mann BK, Tsai AT, Scott-Burden T, West JL. Modification of surfaces with cell adhesion peptides alters extracellular matrix deposition. Biomaterials, 1999; 20: 2281-6.

[23] Staples M, Daniel K, Cima MJ, Langer R. Application of micro- and nano-electromechanical devices to drug delivery. Pharm. Res., 2006; 23: 847-63.
[24] Reed ML, Wu C, Kneller J, Watkins S, Vorp DA, Nadeem A, Weiss LE, Rebello K, Mescher M, Smith AJ, Rosenblum W, Feldman MD. Micromechanical devices for intravascular drug delivery. J. Pharm. Sci., 1998; 87: 1387-94.
[25] Simon DT, Kurup S, Larsson KC, Hori R, Tybrandt K, Goiny M, Jager EW, Berggren M, Canlon B, Richter-Dahlfors A. Organic electronics for precise delivery of neurotransmitters to modulate mammalian sensory function. Nat. Mater., 2009; 8: 742-6.
[26] Sant S, Hancock MJ, Donnelly JP, Iyer D, Khademhosseini A. Biomimetic gradient hydrogels for tissue engineering. Can. J. Chem. Eng., 2010; 88: 899-911.
[27] Singh M, Berkland C, Detamore MS. Strategies and applications for incorporating physical and chemical signal gradients in tissue engineering. Tissue Eng. Pt B-Rev, 2008; 14: 341-366.
[28] Ostrovidov S, Annabi N, Seidi A, Ramalingam M, Dehghani F, Kaji H, Khademhosseini A. Controlled Release of Drugs from Gradient Hydrogels for High-Throughput Analysis of Cell–Drug Interactions. Anal. Chem., 2011; 84: 1302-1309.
[29] Zaari N, Rajagopalan P, Kim SK, Engler AJ, Wong JY. Photopolymerization in Microfluidic Gradient Generators: Microscale Control of Substrate Compliance to Manipulate Cell Response. Adv. Mater., 2004; 16: 2133-2137.
[30] Lo C-M, Wang H-B, Dembo M, Wang Y-l. Cell Movement Is Guided by the Rigidity of the Substrate. Biophys. J., 2000; 79: 144-152.
[31] Justin RT, Engler AJ. Stiffness gradients mimicking in vivo tissue variation regulate mesenchymal stem cell fate. PLOS ONE, 2011; 6: e15978.
[32] Stern E, Jay SM, Demento SL, Murelli RP, Reed MA, Malinski T, Spiegel DA, Mooney DJ, Fahmy TM. Spatiotemporal Control over Molecular Delivery and Cellular Encapsulation from Electropolymerized Micro- and Nanopatterned Surfaces. Adv. Funct. Mater., 2009; 19: 2888-2895.
[33] Li Y, Zhang J, Fang L, Jiang L, Liu W, Wang T, Cui L, Sun H, Yang B. Polymer brush nanopatterns with controllable features for protein pattern applications. J. Mater. Chem., 2012; 22: 25116-25122.
[34] Thissen H, Johnson G, Hartley PG, Kingshott P, Griesser HJ. Two-dimensional patterning of thin coatings for the control of tissue outgrowth. Biomaterials, 2006; 27: 35-43.
[35] Midthun KM, Taylor PG, Newby C, Chatzichristidi M, Petrou PS, Lee J-K, Kakabakos SE, Baird BA, Ober CK. Orthogonal Patterning of Multiple Biomolecules Using an Organic Fluorinated Resist and Imprint Lithography. Biomacromolecules, 2013; 14: 993-1002.
[36] Campbell PG, Miller ED, Fisher GW, Walker LM, Weiss LE. Engineered spatial patterns of FGF-2 immobilized on fibrin direct cell organization. Biomaterials, 2005; 26: 6762-6770.
[37] Saunders RE, Gough JE, Derby B. Delivery of human fibroblast cells by piezoelectric drop-on-demand inkjet printing. Biomaterials, 2008; 29: 193-203.
[38] Chien H-W, Tsai W-B. Fabrication of tunable micropatterned substrates for cell patterning via microcontact printing of polydopamine with poly(ethylene imine)-grafted copolymers. Acta Biomater., 2012; 8: 3678-3686.
[39] Tanaka N, Ota H, Fukumori K, Yamato M, Okano T. Stamp-stiffness calibrated micro contact printing. In: ed.^eds., Robotics and Automation (ICRA), 2013 IEEE International Conference on, 2013; pp. 2582-2587.
[40] DeForest CA, Polizzotti BD, Anseth KS. Sequential click reactions for synthesizing and patterning three-dimensional cell microenvironments. Nat. Mater., 2009; 8: 659-664.

[41] Kuribayashi-Shigetomi K, Onoe H, Takeuchi S. Cell Origami: Self-Folding of Three-Dimensional Cell-Laden Microstructures Driven by Cell Traction Force. PloS one, 2012; 7: e51085.
[42] Park J, Kalinin YV, Kadam S, Randall CL, Gracias DH. Design for a Lithographically Patterned Bioartificial Endocrine Pancreas. Artif. Organs, 2013; 37: 1059-1067.
[43] Drury JL, Mooney DJ. Hydrogels for tissue engineering: scaffold design variables and applications. Biomaterials, 2003; 24: 4337-4351.
[44] Chen F-M, Zhang M, Wu Z-F. Toward delivery of multiple growth factors in tissue engineering. Biomaterials, 2010; 31: 6279-6308.
[45] King WJ, Krebsbach PH. Growth factor delivery: How surface interactions modulate release in vitro and in vivo. Adv. Drug Del. Rev., 2012; 64: 1239-1256.
[46] Yufeng T, Yiyang Z, Yan L, Yumin D. A thermosensitive chitosan/poly(vinyl alcohol) hydrogel containing nanoparticles for drug delivery. Polym. Bull., 2009; 64: 791-804.
[47] Pakulska MM, Vulic K, Shoichet MS. Affinity-based release of chondroitinase ABC from a modified methylcellulose hydrogel. J. Controlled Release, 2013; 171: 11-16.
[48] Song M, Jang H, Lee J, Kim JH, Kim SH, Sun K, Park Y. Regeneration of chronic myocardial infarction by injectable hydrogels containing stem cell homing factor SDF-1 and angiogenic peptide Ac-SDKP. Biomaterials, 2014; 35: 2436-2445.
[49] Jen AC, Wake MC, Mikos AG. Review: Hydrogels for cell immobilization. Biotechnol. Bioeng., 1996; 50: 357-364.
[50] Lee J, Cuddihy MJ, Kotov NA. Three-dimensional cell culture matrices: state of the art. Tissue Eng. Pt B-Rev, 2008; 14: 61-86.
[51] Nicodemus GD, Bryant SJ. Cell encapsulation in biodegradable hydrogels for tissue engineering applications. Tissue Eng. Pt B-Rev, 2008; 14: 149-65.
[52] Wright B, Cave RA, Cook JP, Khutoryanskiy VV, Mi S, Chen B, Leyland M, Connon CJ. Enhanced viability of corneal epithelial cells for efficient transport/storage using a structurally modified calcium alginate hydrogel. Reg. Med., 2012; 7: 295-307.
[53] Li H, Wijekoon A, Leipzig N. Encapsulated Neural Stem Cell Neuronal Differentiation in Fluorinated Methacrylamide Chitosan Hydrogels. Ann. Biomed. Eng., 2014; 42: 1456-1469.
[54] Halstenberg S, Panitch A, Rizzi S, Hall H, Hubbell JA. Biologically Engineered Protein-graft-Poly(ethylene glycol) Hydrogels: A Cell Adhesive and Plasmin-Degradable Biosynthetic Material for Tissue Repair. Biomacromolecules, 2002; 3: 710-723.
[55] Chang Mo H, Shilpa S, Mahdokht M, Nezamoddin NK, Behnam Z, Sang-Hoon L, Ali K. Fabrication of three-dimensional porous cell-laden hydrogel for tissue engineering. Biofabrication, 2010; 2: 035003.
[56] Du M, Zhu Y, Yuan L, Liang H, Mou C, Li X, Sun J, Zhuang Y, Zhang W, Shi Q, Chen B, Dai J. Assembled 3D cell niches in chitosan hydrogel network to mimic extracellular matrix. Colloids Surf. Physicochem. Eng. Aspects, 2013; 434: 78-87.
[57] Du M, Liang H, Mou C, Li X, Sun J, Zhuang Y, Xiao Z, Chen B, Dai J. Regulation of human mesenchymal stem cells differentiation into chondrocytes in extracellular matrix-based hydrogel scaffolds. Colloids Surf. B. Biointerfaces, 2014; 114: 316-323.
[58] Borselli C, Cezar CA, Shvartsman D, Vandenburgh HH, Mooney DJ. The role of multifunctional delivery scaffold in the ability of cultured myoblasts to promote musde regeneration. Biomaterials, 2011; 32: 8905-8914.
[59] Yang C, Mariner PD, Nahreini JN, Anseth KS. Cell-mediated delivery of glucocorticoids from thiol-ene hydrogels. J. Controlled Release, 2012; 162: 612-618.

[60] Guan J, Stankus JJ, Wagner WR. Biodegradable elastomeric scaffolds with basic fibroblast growth factor release. J. Controlled Release, 2007; 120: 70-8.
[61] Davis ME, Hsieh PC, Takahashi T, Song Q, Zhang S, Kamm RD, Grodzinsky AJ, Anversa P, Lee RT. Local myocardial insulin-like growth factor 1 (IGF-1) delivery with biotinylated peptide nanofibers improves cell therapy for myocardial infarction. Proc. Natl. Acad. Sci. USA, 2006; 103: 8155-60.
[62] Gelain F, Unsworth LD, Zhang S. Slow and sustained release of active cytokines from self-assembling peptide scaffolds. J. Controlled Release, 2010; 145: 231-9.
[63] Novajra G, Tonda-Turo C, Vitale-Brovarone C, Ciardelli G, Geuna S, Raimondo S. Novel systems for tailored neurotrophic factor release based on hydrogel and resorbable glass hollow fibers. Mater. Sci. Eng., C, 2014; 36: 25-32.
[64] Bonani W, Motta A, Migliaresi C, Tan W. Biomolecule Gradient in Micropatterned Nanofibrous Scaffold for Spatiotemporal Release. Langmuir, 2012; 28: 13675-13687.
[65] Lee YJ, Lee J-H, Cho H-J, Kim HK, Yoon TR, Shin H. Electrospun fibers immobilized with bone forming peptide-1 derived from BMP7 for guided bone regeneration. Biomaterials, 2013; 34: 5059-5069.
[66] Chakraborty S, Liao IC, Adler A, Leong KW. Electrohydrodynamics: A facile technique to fabricate drug delivery systems. Adv. Drug Del. Rev., 2009; 61: 1043-54.
[67] Lee SS, Huang BJ, Kaltz SR, Sur S, Newcomb CJ, Stock SR, Shah RN, Stupp SI. Bone regeneration with low dose BMP-2 amplified by biomimetic supramolecular nanofibers within collagen scaffolds. Biomaterials, 2013; 34: 452-459.
[68] Meinel L, Kaplan DL. Silk constructs for delivery of musculoskeletal therapeutics. Adv. Drug Del. Rev., 2012; 64: 1111-1122.
[69] Wenk E, Merkle HP, Meinel L. Silk fibroin as a vehicle for drug delivery applications. J. Controlled Release, 2011; 150: 128-141.
[70] Yucel T, Lovett ML, Kaplan DL. Silk-based biomaterials for sustained drug delivery. J. Controlled Release, 2014; 190: 381-397.
[71] Li C, Vepari C, Jin H-J, Kim HJ, Kaplan DL. Electrospun silk-BMP-2 scaffolds for bone tissue engineering. Biomaterials, 2006; 27: 3115-3124.
[72] Mandal BB, Kapoor S, Kundu SC. Silk fibroin/polyacrylamide semi-interpenetrating network hydrogels for controlled drug release. Biomaterials, 2009; 30: 2826-2836.
[73] Onoe H, Okitsu T, Itou A, Kato-Negishi M, Gojo R, Kiriya D, Sato K, Miura S, Iwanaga S, Kuribayashi-Shigetomi K, Matsunaga YT, Shimoyama Y, Takeuchi S. Metre-long cell-laden microfibres exhibit tissue morphologies and functions. Nat. Mater., 2013; 12: 584-590.
[74] Du C, Narayanan K, Leong MF, Wan ACA. Induced pluripotent stem cell-derived hepatocytes and endothelial cells in multi-component hydrogel fibers for liver tissue engineering. Biomaterials, 2014; 35: 6006-6014.
[75] Bosworth LA, Turner L-A, Cartmell SH. State of the art composites comprising electrospun fibres coupled with hydrogels: a review. Nanomed. Nanotechnol. Biol. Med., 2013; 9: 322-335.
[76] Ji Y, Ghosh K, Shu XZ, Li B, Sokolov JC, Prestwich GD, Clark RAF, Rafailovich MH. Electrospun three-dimensional hyaluronic acid nanofibrous scaffolds. Biomaterials, 2006; 27: 3782-3792.
[77] Khadka DB, Haynie DT. Protein- and peptide-based electrospun nanofibers in medical biomaterials. Nanomed. Nanotechnol. Biol. Med., 2012; 8: 1242-1262.
[78] Bhardwaj N, Kundu SC. Electrospinning: A fascinating fiber fabrication technique. Biotechnol. Adv., 2010; 28: 325-347.

[79] Mirahmadi F, Tafazzoli-Shadpour M, Shokrgozar MA, Bonakdar S. Enhanced mechanical properties of thermosensitive chitosan hydrogel by silk fibers for cartilage tissue engineering. Mater. Sci. Eng., C, 2013; 33: 4786-4794.

[80] Xiao W, He J, Nichol JW, Wang L, Hutson CB, Wang B, Du Y, Fan H, Khademhosseini A. Synthesis and characterization of photocrosslinkable gelatin and silk fibroin interpenetrating polymer network hydrogels. Acta Biomater., 2011; 7: 2384-2393.

[81] Du F, Wang H, Zhao W, Li D, Kong D, Yang J, Zhang Y. Gradient nanofibrous chitosan/poly ε-caprolactone scaffolds as extracellular microenvironments for vascular tissue engineering. Biomaterials, 2012; 33: 762-770.

[82] Lee HJ, Koh W-G. Hydrogel Micropattern-Incorporated Fibrous Scaffolds Capable of Sequential Growth Factor Delivery for Enhanced Osteogenesis of hMSCs. ACS Appl. Mater. Interfaces, 2014; 6: 9338-9348.

[83] Manning CN, Schwartz AG, Liu W, Xie J, Havlioglu N, Sakiyama-Elbert SE, Silva MJ, Xia Y, Gelberman RH, Thomopoulos S. Controlled delivery of mesenchymal stem cells and growth factors using a nanofiber scaffold for tendon repair. Acta Biomater., 2013; 9: 6905-6914.

[84] Lee JH, Park J-H, El-Fiqi A, Kim J-H, Yun Y-R, Jang J-H, Han C-M, Lee E-J, Kim H-W. Biointerface control of electrospun fiber scaffolds for bone regeneration: Engineered protein link to mineralized surface. Acta Biomater., 2014; 10: 2750-2761.

1-3 : Échafaudages structurés injectables

L'utilisation d'échafaudages hydrogels a permis d'effectuer de nombreux progrès dans les techniques de médecine régénérative *in vitro.* Malheureusement, les solutions thérapeutiques *in vivo* proposées de nos jours se basent encore principalement, soit sur la croissance de tissu *in vitro* suivie d'une implantation, soit sur l'implantation directe d'un système d'échafaudage. La nécessité d'une chirurgie invasive est contraignante voire impossible dans certains cas et peut entrainer des complications. Les techniques de fabrication d'hydrogels structurés bi/tridimensionnelles encore laborieuses et la volonté de développer une technique de vectorisation non invasive limitent une utilisation *in vivo* optimale [20].

Le développement de techniques simples de fabrication d'hydrogels structurés injectables permettrait d'ouvrir une nouvelle dimension dans la conception de matériaux dits intelligents et le développement de techniques régénératives non-invasives [21-22].

1-4 : Formation d'agrégats à partir de blocs hydrogels

Différentes techniques ont déjà été expérimentées pour induire un assemblage dirigé de blocs hydrogels dans le but de construire un échafaudage [23,24]. La formation d'agrégats peut ainsi être obtenue par une augmentation croissante de la concentration en blocs dans une solution, mais ces techniques posent des problèmes d'organisation des blocs et d'intégrité mécanique [25]. L'utilisation de réseaux microfluidiques peut mener à l'organisation et l'agrégation de blocs mais semble difficile à adapter pour des échafaudages plus grands permettant la croissance de tissus larges [26-28]. La photoréticulation de blocs suspendus à l'interface eau-huile peut permettre le contrôle sur la taille d'un agrégat mais pas sur sa structure [29]. L'utilisation de modèles à base de régions hydrophiles et hydrophobes [30] ou l'utilisation d'imprimante 3D [31]

semble être des voies envisageables pour l'organisation spatiale d'agrégats. Cependant ces techniques ainsi que celles présentées précédemment semblent difficilement applicables dans le but d'obtenir des solutions thérapeutiques injectables et non invasives.

Les hydrogels étant des matériaux facilement fonctionnalisés, la voie privilégiée pour développer de telles solutions thérapeutiques semblent celles basées sur des interactions adhésives entre blocs. Ainsi, des blocs hydrogels peuvent être synthétisés et fonctionnalisés de telle manière à promouvoir des interactions adhésives avec les blocs environnants. Différents types de fonctionnalisations et de mécanismes ont déjà été expérimentés : addition de Michael entre groupes réactifs à la surface des blocs [32], interactions moléculaires à l'aide d'interactions ligand-récepteur [33,34], chaînes ADN complémentaires incorporé aux blocs hydrogels [35], nucléation et croissance de fibres de collagène aux interfaces [36]. Il a de plus été démontré que la fonctionnalisation à l'aide de polymères ou de nanoparticules entrainait l'apparition de propriétés adhésives entre surfaces hydrogels [37-40].

Chapitre 2 : Objectifs et méthodologie

2-1 : Objectifs

Nous pensons qu'il est possible de développer une solution thérapeutique de médecine régénérative en développant une matrice hydrogel structurée injectable se basant sur les propriétés adhésives que nous pouvons induire par fonctionnalisation électrostatique de blocs hydrogels.

Ce projet de recherche développe un procédé de fabrication simple de matrices d'hydrogel micro-structurées et injectables. Le procédé proposé utilise des blocs préfabriqués d'hydrogel fonctionnalisés électrostatiquement qui formeront, via un procédé d'assemblage dirigé, une

matrice complexe dont la structure pourra être prédéfinie par la géométrie et la fonctionnalisation des blocs qui la composent.

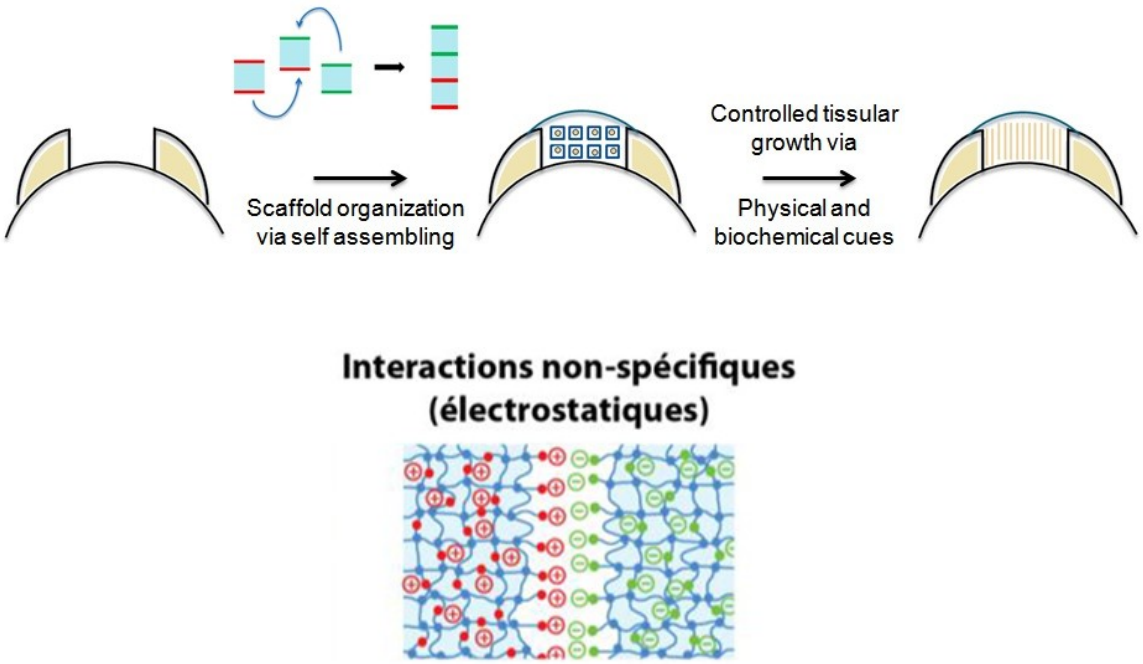

Figure 2-1 : Principe de la croissance contrôlée de néo-tissus à l'aide d'un échafaudage hydrogel formé par l'assemblage dirigé de blocs hydrogels injectables fonctionnalisés électrostatiquement

Notre projet se découpe en trois objectifs principaux :

- Le développement d'une technique de fabrication de blocs hydrogels de forme et taille contrôlées
- La fonctionnalisation électrostatique des blocs à l'aide de polyélectrolytes et de microgels chargés
- L'étude des interactions adhésives et des propriétés d'auto-assemblage dans différents milieux aqueux (salinité, pH)

2-2 : Méthodologie

2-2-1 : Fabrication de blocs hydrogels

Notre objectif premier étant le développement d'une technique de synthèse simple et répétable de blocs hydrogels de forme et taille contrôlée, divers procédés ont été envisagés et testés. Nous avons tout d'abord envisagé l'utilisation de moules. Ces moules auraient pu directement représenter la forme des blocs voulus ou bien la forme d'un pain d'hydrogel qu'il nous aurait suffi de découper à l'aide d'une lame (Figure 2-2). Des négatifs de moules en téflon ont ainsi été obtenus à l'aide d'une machine de fraisage contrôlée par ordinateur. Ces négatifs étaient ensuite utilisés en versant une solution de précurseurs puis placés sous une lampe UV pour obtenir des moules en polydiméthylsiloxane (PDMS). Les moules en PDMS étaient ensuite remplis de la solution de précurseur hydrogel et recouverts d'une lame de verre avant d'être placés sous la lampe UV pour photopolymérisation. Cette voie de synthèse a cependant été abandonnée. D'une part des problèmes de fuite de solution étaient régulièrement constatés et, d'autre part, les blocs hydrogels obtenus présentaient des défauts de surface à l'endroit du contact avec le moule.

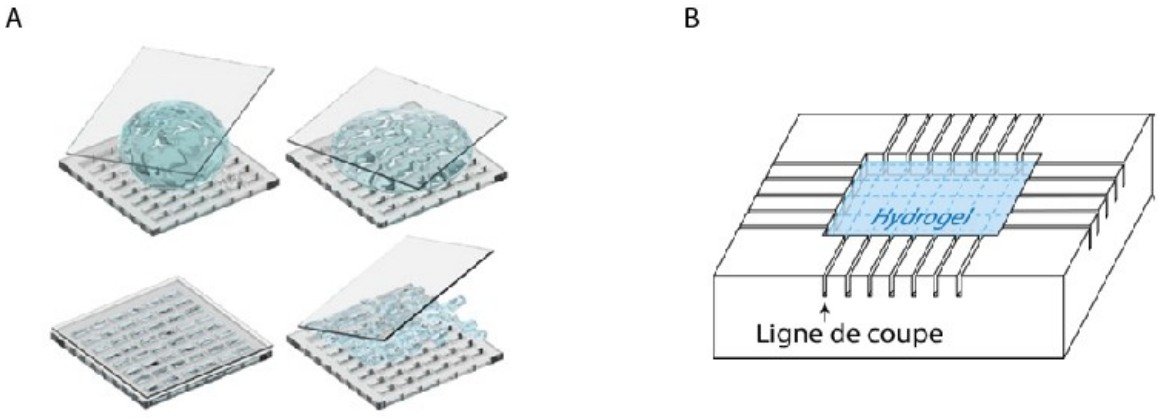

Figure 2-2 : Principe de l'utilisation de moules A) Pour obtenir des blocs B) Pour obtenir un pain d'hydrogel pouvant être découpé

Nous avons donc décidé de changer de voie de synthèse et de nous intéresser à l'utilisation de photomasques. Pour cela nous avons construits différents support d'injection composés de deux lames de verres positionnées l'une au-dessus de l'autre à l'aide d'espaceurs de taille connue. Il est ainsi possible d'injecter notre liquide entre les lames de verres sans écoulements par capillarité. Le dispositif est complété par l'impression de photomasques aux dimensions des blocs voulus sur du papier transparent. Le photomasque est déposé sur le support d'injection et maintenu en place à l'aide d'une autre lame de verre déposée dessus (Figure 2-3).

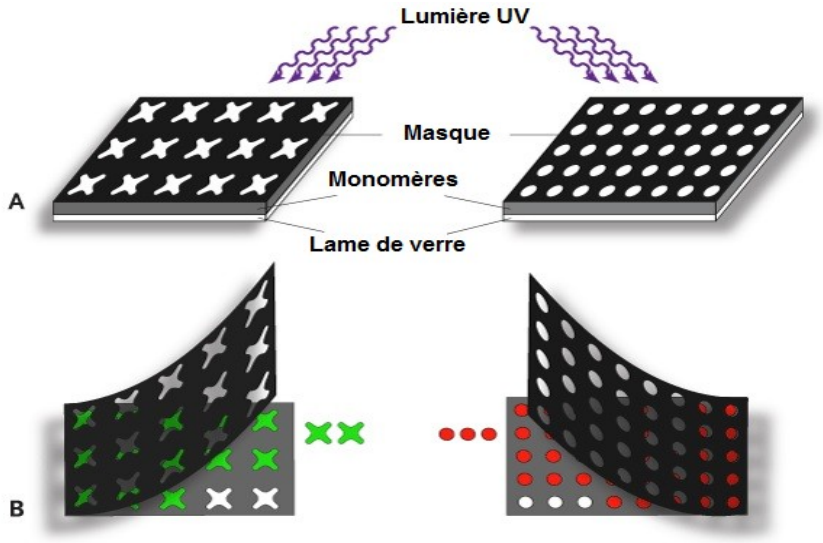

Figure 2-3 : Principe de l'utilisation de photomasques pour la synthèse de blocs de forme et taille contrôlées

Cette technique nous a permis d'obtenir des blocs de formes différentes (Figure 2-4) avec des dimensions de 2x2mm et des épaisseurs variant entre 0.15mm et 3mm, même si des problèmes de repliement ont été observés pour les épaisseurs les plus fines.

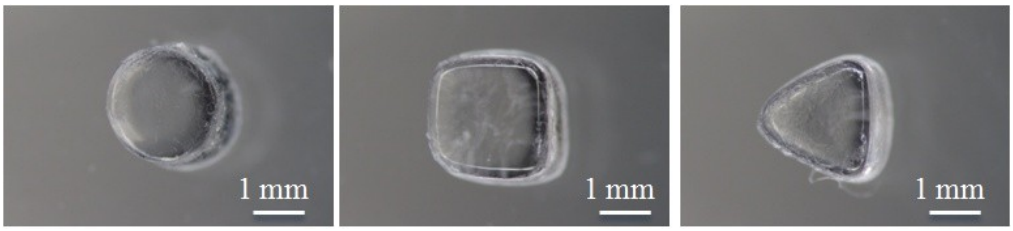

Figure 2-4 : Différentes formes de blocs obtenues à l'aide du support d'injection et des photomasques

2-2-2 : Fonctionnalisation des blocs hydrogels

La formulation d'hydrogel dont nous nous sommes servis est un mélange (hydroxyéthyl)méthacrylate-poly(éthylène glycol diméthacrylate) déjà utilisé en sciences biopharmaceutiques [41]. Ces hydrogels présentent des propriétés de gonflement très faibles, ce qui nous permet de nous assurer de conserver la forme des blocs, tout en présentant des pourcentages en eau assez élevés (de l'ordre de 40-50%). Ils sont obtenus par dissolution des précurseurs dans l'eau avec, comme photoinitiateur, de l'Irgacure 2959. La solution est ensuite injectée dans le support que nous avons développé puis le tout est placé sous lampe UV.

Comme nous avons décidé d'étudier l'assemblage dirigé des blocs à l'aide d'interactions électrostatiques, nous avons utilisés des polyélectrolytes chargés positivement et négativement ainsi que des microgels chargés négativement pour fonctionnaliser nos hydrogels. Pour l'obtention de blocs positifs, après avoir effectué des tests peu concluant en utilisant du poly(allylamine), nous nous sommes fixés sur l'utilisation de PEI branché. Le PEI est ajouté à la solution de précurseur qui est légèrement chauffé pour permettre sa dissolution. La photopolymérisation est ensuite effectuée de la même manière que pour les blocs neutres.

De manière similaire, des blocs chargés négativement ont été obtenus par ajout d'un polyanion, l'acide hyaluronique, déjà largement utilisé en sciences biopharmaceutiques. Enfin, un second

type de blocs négatifs a été développé à l'aide de microgels chargés négativement. Nous avons ainsi traité des blocs PEI positifs avec des microgels NIPAM-MAA chargés négativement. De tels microgels avec différents % de MAA avait été développés et étudiés précédemment par mon collègue Pierre-Luc Latreille lors de son master qui s'était intéressé à leur potentiel en tant que cargo pour le relargage contrôlé de composés actifs.

2-2-3 : Tests d'assemblage

Les tests d'assemblage consistent à la mise en contact aléatoire de mélange de blocs positifs et négatifs. Pour cela, nous avons décidé d'utiliser des petits cristallisoirs remplis comme contenant, permettant une bonne suspension des blocs, et un agitateur orbitalaire pour la mise en mouvement des blocs. Nous nous sommes fixés sur des blocs d'une taille de 2x2x1 mm^3. Après plusieurs tests avec différentes tailles de population, nous avons défini notre test standard avec une population de 2x5 cubes. Les tests ont été effectués dans des cristallisoirs remplis de 10mL de solution aqueuse.

Chapitre 3: Résultats

L'ensemble des résultats d'assemblage dirigé obtenus pour les deux systèmes dans différents milieux aqueux a été compilé dans l'article présenté ci-dessous. Ce dernier a été soumis pour publication dans le journal Langmuir (en cours de révision à date du 1er Mars 2017)

Artide 2: **Assembly of hydrogel blocks mediated by polyelectrolytes or microgels: effect of salinity, pH and microgel surface charge**

Nicolas Hanauer, Pierre Luc Latreille, Xavier Banquy

Canada Research Chair in Bio-inspired Materials and Interfaces, Faculty of Pharmacy, Université de Montréal C.P. 6128, Succursale Centre Ville, Montréal, QC H3C 3J7, Canada

Rôle des auteurs

La formulation et la préparation des microgels NIPAM-MAA ont été effectuées par Pierre-Luc Latreille, qui avait déjà étudié leur potentiel comme système de livraison contrôlée. J'ai réalisé le reste des expériences présentées et effectué la rédaction. L'ensemble des expériences ont été conduite sous la supervision du Pr Banquy.

Résumé en français

Dans cet article, nous étudions l'assemblage dirigé de blocs hydrogels à l'aide d'interactions électrostatiques. Nous avons comparé deux mécanismes d'assemblage différents, l'un basé sur des particules microgel et l'autre basé sur des interactions directes entre blocs de charge opposée. Le système consiste en des blocs d'hydrogel composé d'un réseau interpénétré d'(hydroxyethyl)méthacrylate-poly(éthyleneglycol)diméthacrylate (HEMA-PEGDMA) et soit de polyéthylèneimine (PEI) chargé positivement soit d'acide hyaluronique (HA) chargé négativement. Les blocs chargés positivement ont été prétraités avec des particules microgel chargés (MG) composé de N-isopropylacrylamide-acide méthacrylique. Les deux systèmes (PEI/HA et PEI/MG) ont présenté des propriétés d'assemblage dirigé, signifiant que les blocs positifs ont été systématiquement trouvés en contact avec des blocs négatifs. Dans l'eau, les agrégats obtenus par assemblage dirigé étaient plus larges et fragiles pour PEI/HA et plus

compacts et résistants pour PEI/MG. L'effet du sel et du pH a été étudié pour les deux systèmes. L'inhibition de l'agrégation des blocs a été observé au-dessus d'une concentration en sel critique (C^*_{Salt}) significativement plus élevé pour le système PEI/HA (80mM) que pour le système PEI/MG (5-20mM). Nous avons aussi observé que (C^*_{Salt}) augmentait avec le % de MAA dans les microgels et avec la concentration de la suspension de microgel (C_{MG})utilisé pour traiter la surface des blocs hydrogels. Aucun assemblage dirigé n'a été observé pour les deux systèmes en conditions acide et basiques (pH=3 et 10.5). Nos résultats mettent en lumière les différences subtiles dans les mécanismes d'adhésion entre blocs et montre la voie pour le design innovant de nouveaux matériaux mous complexes.

Abstract

In this study, we studied the directed assembly of hydrogel blocks mediated by electrostatic interactions. We compared two different assembly mechanisms, one mediated by microgel particles and one mediated by direct interaction between oppositely charged blocks. The system consisted in hydrogel blocks made of an interpenetrated network of (hydroxyethyl)methacrylate-poly(ethyleneglycol)dimethacrylate (HEMA-PEGDMA) and either positively charged polyethyleneimine (PEI) or negatively charged hyaluronic acid (HA). Positively charged hydrogel blocks were pretreated with negatively charged microgel particles (MG) made of N-isopropylacrylamide-methacrylic acid. Both systems (PEI/HA and PEI/MG) demonstrated directed assembly, meaning that positive blocks were systematically found in contact with oppositely charged blocks. Directed assembly in water resulted in large and fragile PEI/HA aggregates compared to more compact and resistant PEI/MG aggregates. Effects of salt and pH were also assessed for both systems. Inhibition of blocks aggregation was found to appear above a critical salt concentration (C^*_{Salt}) which was significantly higher for PEI/HA (80 mM)

compared to PEI/MG (5-20mM). C^*_{Salt} was also found to increase with the % of MAA in the microgels and with the concentration of the microgel suspension (C_{MG}) used to treat the hydrogel block surfaces. No directed assembly was observed in acidic and basic media (pH = 3 and 10.5) for both systems. Our results shine light on the subtle differences underlying the adhesion mechanisms between hydrogel blocks and suggest new routes toward the design of innovative complex soft materials.

Keywords: hydrogel block, microgels, polyelectrolytes, directed assembly, adhesion

Introduction

Hydrogels, composed of a polymeric matrix and an "immobilized" liquid phase, are ideal materials for bioengineering[1]. On one hand, their polymeric structures are highly versatile and tunable in terms of physical (swelling, stiffness, porosity…) and chemical modifications (functionalizations, sensitivity to environmental cues…). On the other hand, the trapped liquid phase can be used to load and preserve various active compounds (chemical species, growth factors, cells….) in the polymeric network. Since hydrogel matrices are highly tunable, they offer the possibility to design matrices with finely tuned structural environment which in turn can direct the fate of the species they carry [2]. These unique properties have initially been used to develop cargos for drug delivery systems[3, 4]. For example, cell-seeded hydrogel scaffolds with various internal cues are now the prime techniques used for regeneration of various tissues (skin [5, 6], cartilage [7, 8], bones[9]…)

In addition, to gain a finer control over the microenvironment inside these hydrogel matrices, assembly techniques are being used[10]. *In situ* polymerization seems the easiest path to follow,

since many different polymeric interactions can lead to hydrogel formation: chemical crosslinking[11, 12], electrostatic interactions[13, 14], complementary binding[15, 16]. Injection of reagents, with or without active compounds, can result in hydrogel synthesis triggered by stimuli (temperature, pH…) or by mixing. Such techniques are limited by physiological conditions, toxicity of the injected components and, moreover, by the poor control over hydrogel structure and active compounds loading conditions. Similarly, poor control over structure and loadings restrict the use of hydrogel scaffolds for regenerative medicine.

Another approach to obtain *in situ* hydrogel matrices with controlled architecture is using the directed assembly of prefabricated hydrogel blocks[17, 18]. This bottom-up approach could possibly offer a better control over the three dimensional distribution of embedded active compounds. This approach might unlock new possibilities of combining a large spectrum of mechanical and biochemical cues within a defined hydrogel scaffold. This would simply require selecting formulations and functionalizations needed in separate blocks to design the desired scaffold. It might also be a powerful approach to program a predefined structure to mimic the bio-functional organization of a tissue.

Different experimental techniques have been proposed for the directed assembly of hydrogel blocks. Blocks aggregation via concentration increase can lead to the formation of aggregates but the lack of control over blocks organization and mechanical integrity is a concern[19]. Microfluidic devices can produce selective aggregation of a few blocks but seems more difficult to adapt for larger, tissues-sized, aggregates[20, 21, 22]. Stabilization of blocks in water-in-oil droplets followed by secondary photo crosslinking allows control over size of the aggregate but not over its final structure[23]. Using templates with hydrophobic and hydrophilic regions is a method to guide blocks organization on a patterned surface but is challenging to translate into 3D structures[24]. Tissue printing is a promising solution towards 3D organization of cell-laden

hydrogels but it is still more suitable for layered materials than for injectable blocks[25]. Other fabrication techniques have also been proposed via incorporation of magnetic cues [26].

Nevertheless, as hydrogels are easily tunable, the most widely used approach is based on block-block interactions, especially to promote directed assembly. Hydrogel blocks can be designed to interact and adhere specifically with neighboring blocks. A wide spectrum of adhesive mechanisms have been tested: Michael type addition between reactive groups at blocks surfaces[27], molecular recognition via host-guest interactions[28, 29], complementary DNA chains incorporated in the hydrogel block[30], nucleation and growth of collagen fibers at interfaces [31]. These techniques make use of a wide variety of adhesion mechanisms, resulting in promising hydrogel assemblies. Furthermore, it has been proved that surface modification with polymers brushes or nanoparticles can also efficiently promote adhesion between soft surfaces[32, 33, 34, 35].

In this report, we have studied the assembly of hydrogel blocks mediated by electrostatic interactions. We studied two different interaction mechanisms, one where hydrogel blocks assembly is mediated by direct contact between oppositely charged blocks and a second mechanism where assembly between identical blocks is mediated by oppositely charged microgel particles (MG). The hydrogel blocks were fabricated by UV photolithography in presence of different polyelectrolytes (PEI or HA). Since electrostatic forces were expected to drive the blocks assembly, we studied the effect of pH, ionic strength and microgel composition to elucidate differences between the two interaction mechanisms.

Materials and methods:

Materials

2-hydroxyethyl methacrylate (HEMA, 97%), poly(ethylene glycol)dimethacrylate (PEGDMA, Mn = 550g/mol), N,N'-methylenebis(acrylamide) (BisA, 99%), N-Isopropylacrylamide (NIPAM, >99%),

sodium dodecyl sulfate (SDS, >98.5%), methacrylic acid (MAA, 99%) hydrochloric acid (HCl, 37%) and aluminum oxide (activate, basic, Brockmann I) were purchased from Sigma-Aldrich Canada, Ltd. (Oakville, Canada). Irgacure 2959 was a kind gift from BASF (Mississauga, Canada). Polyethyleneimine (PEI, branched, Mw = 10 000g/mol, 99% purity) was from Alfa Aesar (Ward Hill, USA). Sodium hyaluronate (HA, Mw = 60 000 g/mol) was purchased from LifeCore Biomedical (Chaska, USA). Sodium chloride (NaCl) and ammonium persulfate (APS) were from Fisher Chemical (Ottawa, Canada). Unless stated, materials were used without prior purification.

Hydrogel blocks preparation

Blank hydrogel blocks were obtained via photopolymerization of HEMA using PEGDMA as a cross-linker. After their purification on a basic aluminum oxide column, a mixture of HEMA-PEGDMA (99.8:0.2 mol%) was dissolved in water (65 wt%) for 10min under magnetic stirring. Irgacure 2959 was then added as photoinitiator (5 wt% total). The mixture was then placed under high intensity UV lamp (UVP Mercury Spot Low, 100MW Longwave) for 30min.

Hydrogel solutions were injected in a mold composed of two glass slides separated by a glass spacer. The loaded mold was then covered with a photomask and another glass slide. The photomasks consisted of a printable transparent slide imprinted with the desired arrangement of squares. With this technique, we were able to shape hydrogel blocks of size larger than 1mm and thickness ranging between 0.15mm to 3mm depending on the thickness of the spacer used. After polymerization, the injection mold was opened, the unreacted mixture was washed away with water under pressure and the blocks were gently separated from the glass plates with a spatula. Blocks were then kept in water (~25 blocks/10mL) under high magnetic stirring to ensure complete swelling and removal of unreacted monomers.

Positively charged hydrogel blocks were obtained by adding polycationic PEI (25 wt%) prior to the photopolymerization step. PEI was added to the HEMA-PEGDMA mixture and then dissolved in water at around 40°C, allowing for the complete dissolution of PEI. PEI blocks were colored in red by adding a few droplets of a Rhodamine 6G solution (0.5mg/mL) in the monomer mixture before polymerization. Similarly, in order to obtain negatively charged blocks, an anionic polyelectrolyte was added to the reagents mixture prior to photopolymerization. A HA solution (3mg/mL) was prepared one day prior to photopolymerization in a water and HCl mixture (6.6 vol%). This HA solution was used to mix the monomer solution of HEMA and PEG-DMA at a final concentration of 35 wt%. HA blocks were colored in blue using a food coloring dye before polymerization.

An alternative procedure used to produce negatively charged blocks was to treat positively charged blocks with a solution of negatively charged NIPAM-MAA microgels. Blocks were immersed in a MG solution at C_{MG}= 4mg/mL (25 blocks/10mL, 24 hours) under magnetic stirring and then rinsed in water for 1 hour to eliminate non adsorbed microgels.

Microgels preparation

NIPAM-MAA microgels used in this study were synthesized by precipitation polymerization. Briefly, monomers (NIPAM with MAA at 0, 5, 10 or 20 mol%), BisA as cross-linker (5mol% total monomers) and SDS (867µmol/L) as surfactant were dissolved in degassed water. The mixture was then placed at 65°C under mechanical stirring (200 rpm) and argon atmosphere for equilibration. APS (2.9 mmol/L) was then injected in the reaction vessel. Polymerization was let to proceed during 4h30 at a temperature of 75°C and constant stirring of 300 rpm. The resulting particle solution was then dialyzed (Spectra/Por Tube-A-Lyzer Dynamic Dialysis Device, 100 kDa MWCO) against milliQ water (~60mL of particle suspension for 20L of water, overnight). Four

batches of microgels were synthesized containing 0 to 20 % of MAA.C_{MG}in the final suspension was determined by lyophilizing a volume of1.5 mL of suspension. Size, polydispersity and ζ potential of the MG particles (100-800µg/mL) in water and with various salt concentrations at 22°C were characterized via dynamic and phase analysis light scatterings (DLS and PALS) using a Brookhaven NanoBrook Omni (90° detection angle, illumination wavelength 640nm). The microgels surface potential was found to be negative independently of the MAA content. Since the polymerization of NIPAM was initiated by ammonium persulfate which is negatively charged in solution, the polymer chain ends bearing the initiator moiety are expected to provide negative charges at the surface of the microgel even at 0% of MAA.

Directed assembly tests

Tests were performed in small crystallizers filled with 10mLof distilled water. Mixtures of positively and negatively charged 2x2x1mm^3 blocks were suspended together under constant mixing conditions with an orbital shaker (150-200 RPM, 3min) until completion of the assembly process. Upon completion of the assembly process, aggregates were imaged and counted. All the assembly tests were carried out in quintuplet to insure proper statistical robustness. Cycles of assembly and disassembly were performed during each test to evaluate surface integrity and directed assembly robustness under mechanical stresses. Once an aggregation test is performed, the cubes are gently separated using a spatula before starting another experiment. When the adhesion between the cubes was weak, gentle manipulation without inserting the spatula in between the cubes was sufficient to separate them. The reformed block suspension was immediately retested on the orbital shaker. Each test was repeated at least three times and results show average values only.

Effect of C_{Salt} and pH were also studied. Salinity of the media was controlled using NaCl. In such cases, blocks were left 10min or 24h to equilibrate in the NaCl solutions (25 blocks/10mL) before testing their assembly in freshly prepared saline medium.

Assembly tests under acidic or basic conditions were achieved using similar protocol with HCl and NaOH solutions (pH =3 and 10.5, 24h equilibrium). Imaging of the blocks and aggregates was performed on a Zeiss Stereo Discovery V8 stereomicroscope under high illumination. During observation, the samples were immersed in water in a small crystallizer.

Results

For both types of systems, i.e. oppositely charged blocks (PEI/HA) or blocks pretreated with microgels (PEI/MG) we were able to observe directed assembly, meaning that we obtained, after agitation of the block ensemble, aggregates that could resist to gentle spatula manipulation (see Fig. 1). Even if we observed the assembly of blocks for both systems, macroscopic observations of the aggregates seemed to demonstrate that two types of adhesion mechanisms are involved. PEI/HA aggregates were indeed larger in size and deformable but also more fragile than the more compact PEI/MG aggregates. These differences in aggregate structure were even more important with aggregates of 10 blocks (See Figure 1). Aggregates between HA and PEI were formed of adhesive contacts between identically charged surfaces were also observed. Tests with blocks of the same type (HA/HA, PEI/PEI and PEI/MG-PEI/MG) did not lead to the obtention of significant directed assembly properties. Moreover, control tests using HA, PEI and PEI-MG blocks with neutral HEMA-PEGDMA hydrogel blocks did not lead to any aggregate formation.

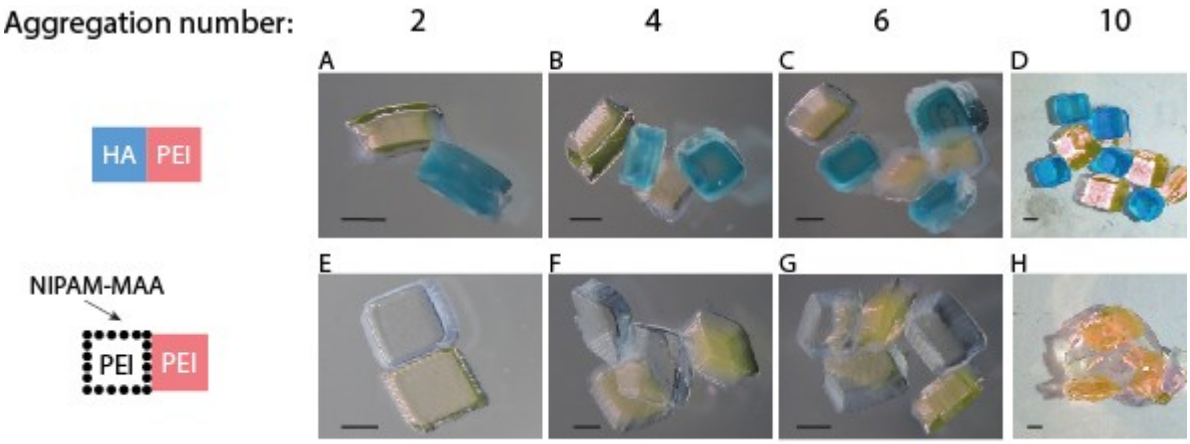

Figure 3-1: Stereomicroscopies (A, B, C, E, F, G) and camera pictures (D, H) of PEI/HA and PEI/MG aggregates of different sizes (scale bar: 1mm)

A more quantitative analysis of the directed assembly tests is presented in Figures 2 and 3. In these figures, we show the cumulative % of aggregated blocks versus the number of blocks per aggregate (aggregation number) and the average aggregation number as a function of the iteration.

Both systems were tested under different conditions to investigate their properties and differences. The first test aimed to study the effect of population sizefor the PEI/HA system, i.e. the effect of blocks concentration on aggregates size maintaining the ratio between block partners equal to 1. We have chosen to study three PEI/HA blocks populations: 3:3, 5:5 and 10:10 for 5 iterations of assembly-disassembly. In Figure 2A-C, we represent the cumulative percentage of aggregated cubes as a function of the aggregation number. The data should be read as follow: the cumulative percentage represents the fraction of blocks in aggregates of a given aggregation number (number of blocks per aggregate) or less. In this representation, a cumulative percentage of 100% for an aggregation number of 4 means that 100% of the cubes are part of aggregates of 4 blocks or less. A group of unaggregated blocks will be represented by a straight horizontal line located at 100% starting at an aggregation number equal to 1 (see Figure 3A). A group of 10 blocks forming one single aggregate of 10 blocks will be represented

by a straight horizontal line starting at 0% below an aggregation number equal to 10 and going to 100% above 10. We observed that an increase of the block population size led to larger aggregates at the first iteration (the cumulative percentage reaches 100% at a high aggregation number). For example, the 10:10 population exhibited large aggregates only (> 17 blocks) after the first aggregation test while the 3:3 and 5:5 populations lead to a mixture of mid-sized aggregates (4 to 6 blocks per aggregates). For the three tested populations, the average aggregates size was significantly reduced after the first assembly-disassembly iteration and continued to gradually decrease until 5 iterations were performed (Fig. 2D-F).

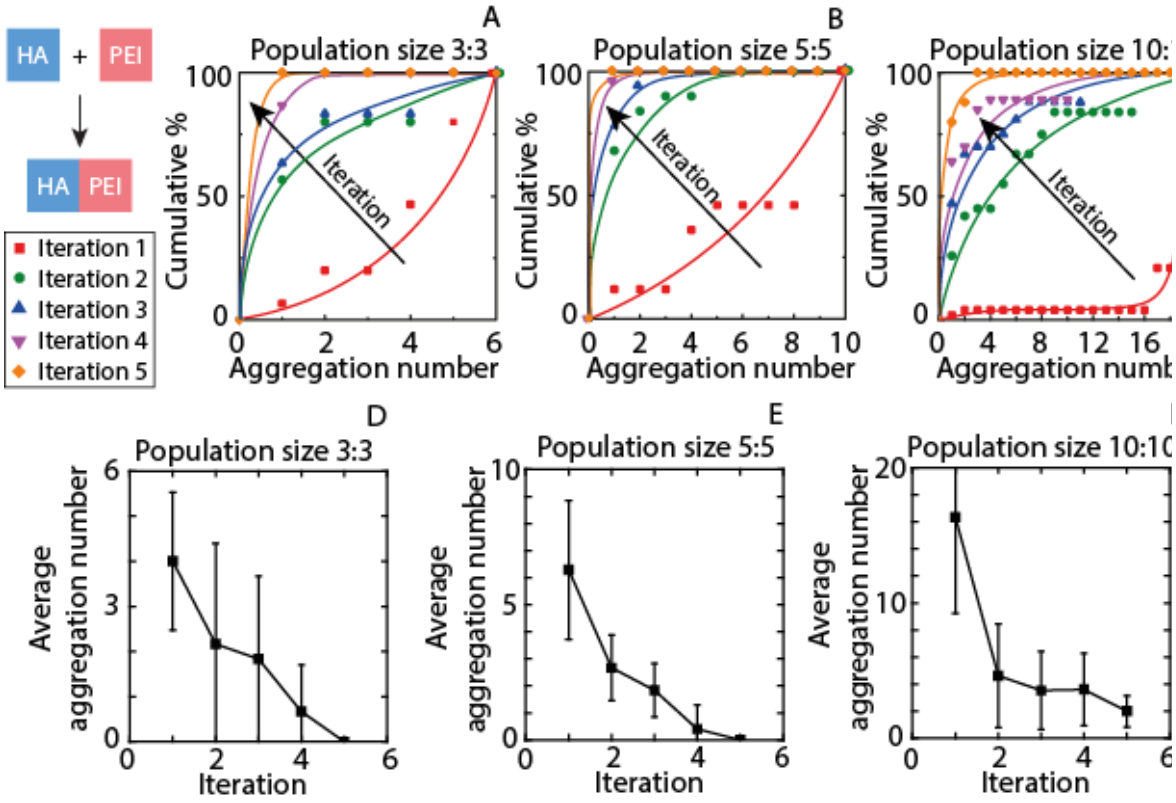

Figure 3-2: A) to C): Cumulative % of blocks aggregation as a function of the aggregation number (number of blocks per aggregates. D) to F): Average aggregation number as a function of the experiment iteration. Lines are guides for the eye.

The PEI/MG system demonstrated strong directed assembly properties, especially for smaller block populations, (5:5 and lower). Therefore, we fixed the block population size to 5:5 for the remaining experiments.

In the PEI/MG system, PEI blocks pretreated with MG and mixed with untreated PEI blocks. We tested 4 types of microgels with increasing MAA content (See Table 1) and studied the directed assembly of the hydrogel blocks after pretreatment with these microgels(C_{MG} = 4mg/mL, 25 blocks/ 10mL, 24 hours). We used a block population size of 5:5 and performed 3 assembly-disassembly iterations for each test (see Figure 3).

While pretreatment with MAA0% microgels did not lead to any aggregation (Fig. 3A), Fig. 3B-D shows that pretreatments with the three other types of microgels (MAA5%, 10% and 20%) lead to the formation of large aggregates at the first iteration (8, 9, 10 blocks per aggregate). Increasing the number of assembly/disassembly cycle slightly decreased the aggregates size but did not inhibited their formation as previously observed with PEI/HA blocks (Fig. 3E).

MAA%	d (nm)	ζ-potential (mV)
0%	211.6±1.4	-14,3±0,9
5%	303.1±2.8	-23,8±1,1
10%	375.0±3.8	-27,2±0,8
20%	557.1±4.4	-29,3±1,3

Table 1: Particle size and ζ-potential of the NIPAM-MAA microgels

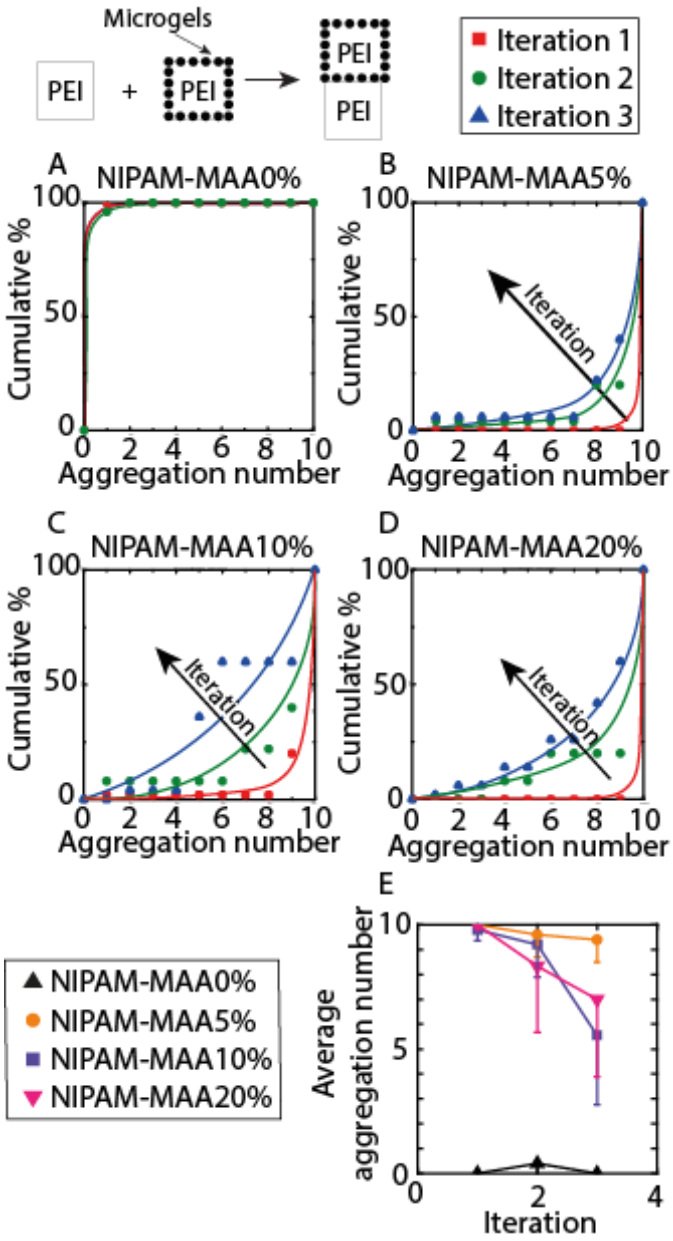

Figure 3-3: Effect of the MAA content in microgels on the directed assembly of PEI containing hydrogel blocks. A) to D) Cumulative % of blocks aggregation as a function of the aggregation number (number of blocks per aggregates). E) Average aggregation number as a function of the experiment iteration. Curves are guides for the eye.

In Figure 3, the pretreatments of the PEI blocks with the MG were conducted at C_{MG}= 4mg/mL which we supposed was above the concentration necessary to reach saturation of the block surfaces. To confirm this hypothesis, we tested different values of C_{MG} for all the MG (MAA5%, 10% and 20%) ranging from 0.008mg/mL to 8mg/mL (Figure 4). In Figure 4A, the total

aggregation% (the total number of aggregated blocks independently of the aggregate size) is represented versus the calculated MAA concentration of the microgel suspension during pretreatment (C_{MAA}). We observed that aggregation of the hydrogel blocks did not occur below a critical concentration,C^*_{MAA}, which increased with the MAA content in the microgels, from 2.9µg/mL for MAA5% to 11.7µg/mL for MAA20%. Interestingly, these values of C^*_{MAA} corresponded to a critical microgel concentration, C^*_{MG} = 0.04 mg/mL for all the MG. One possible explanation of such behavior is that the microgel size increases significantly with MAA% without any significant changes in zeta potential. Therefore most of the MAA is expected to be located inside the microgel particle and not at its surface. Consequently, the charge surface density is expected to decrease with the MAA% in the microgel which could explain why C_{MAA}* increases with MAA%.

In Figure 4B-D, we represent the results of the assembly tests in terms of cumulative aggregation %, which depends on the size of the aggregates. In these panels, the indicated concentration of microgels corresponds to the microgel concentration in the pretreatment suspension. We noticed that the system pretreated with the MAA20% microgels at 0.08mg/mL presented significantly smaller aggregates compared to all the other systems at the sameC_{MG}. Figure 4E displays the average aggregation number obtained with the MAA5% microgels pretreatment as a function of the experiment iteration for each microgel concentration used. Results show a quasi-constant (or slightly decreasing) average aggregation number for C_{MG}> 0,08mg/mL and complete loss of of blocks aggregation when C_{MG}< 0.08 mg/mL. Results were identical for MAA10% and 20% microgel pretreatments (data not shown). Observation of a similar aggregate distribution and average aggregation number at C_{MG} superior to 0.08mg/ml, independently of the MAA content in the microgels, tends to confirm that the microgel saturation concentration was reached at these concentrations.

It is worth noting that for all the C_{MG} tested, we did not observe any directed assembly of the blocks during the pretreatment test, which means that the observed assembly could only be obtained between treated and non-treated blocks only.

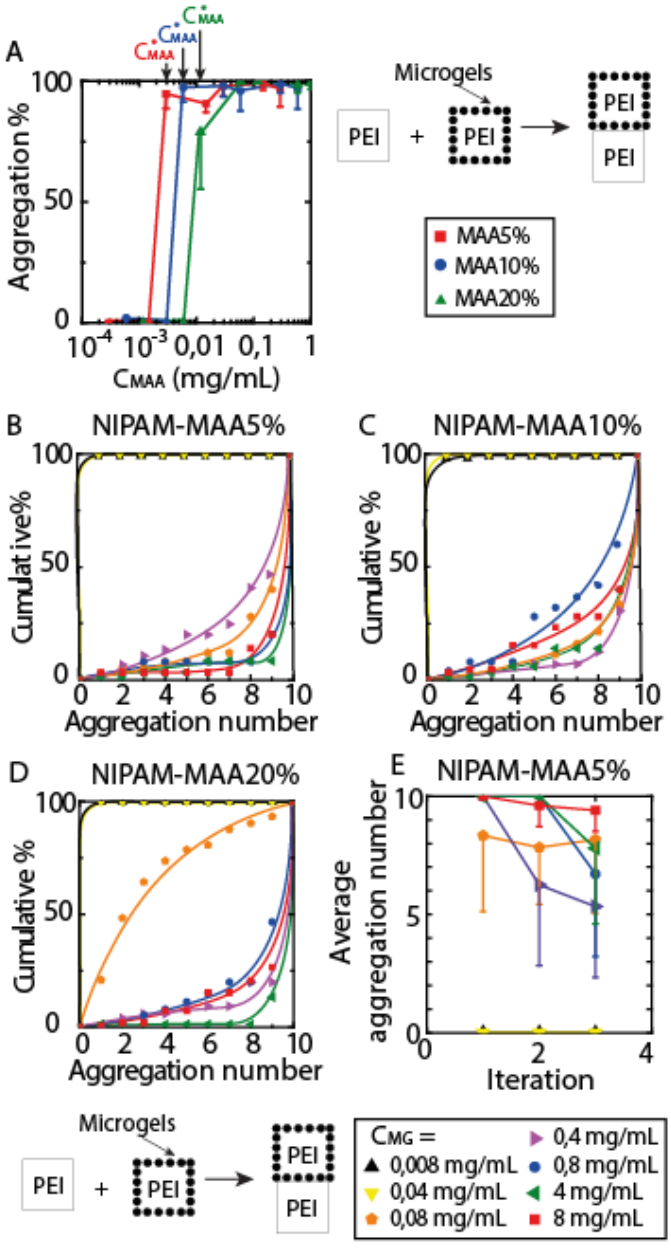

Figure 3-4: Effect of the microgel concentration on the directed assembly of PEI blocks. (A) Blocks aggregation % as a function of MAA content in the microgels during the pretreatment. B-D) Cumulative % of aggregated blocks as a function of the average aggregation number (represented values are averages of three assembly iterations). E) Average blocks aggregation number in presence of NIPAM-MAA5% microgels only. Error bars represent the standard deviation of 5 separate experiments. Lines are guides for the eye.

To explore the role played by electrostatic forces in the assembly of the hydrogel blocks, we performed a series of tests at increasing salt concentrations (C_{Salt} = 0-150mM NaCl, see Figure 5A). Above a critical salt concentration,C^*_{Salt}, the aggregation of the hydrogel blocks was strongly hampered, independently of the system. PEI/HA blocks were found to resist significantly more to the increase in salinity (C^*_{Salt} = 80 mM), even after prolonged incubation in saline solution (24h) compared to PEI/MG systems. The value of C^*_{Salt} was found to depend on the MG composition, and increased with MAA content, from C^*_{Salt} = 5mM for MAA5% to C^*_{Salt} = 20mM for MAA20%. The value of C^*_{Salt} was also found to depend on the C_{MG}(See Figure 5B). While pretreatments with C_{MG} = 8 and 4mg/mL presented similar behavior (C^*_{Salt} =20mM), a decrease in C^*_{Salt} was observed at C_{MG} = 0.4mg/mL (C^*_{Salt} = 10mM) until almost complete loss of directed assembly was observed at C_{MG} = 0.08mg/mL (C^*_{Salt} = 2.5mM).

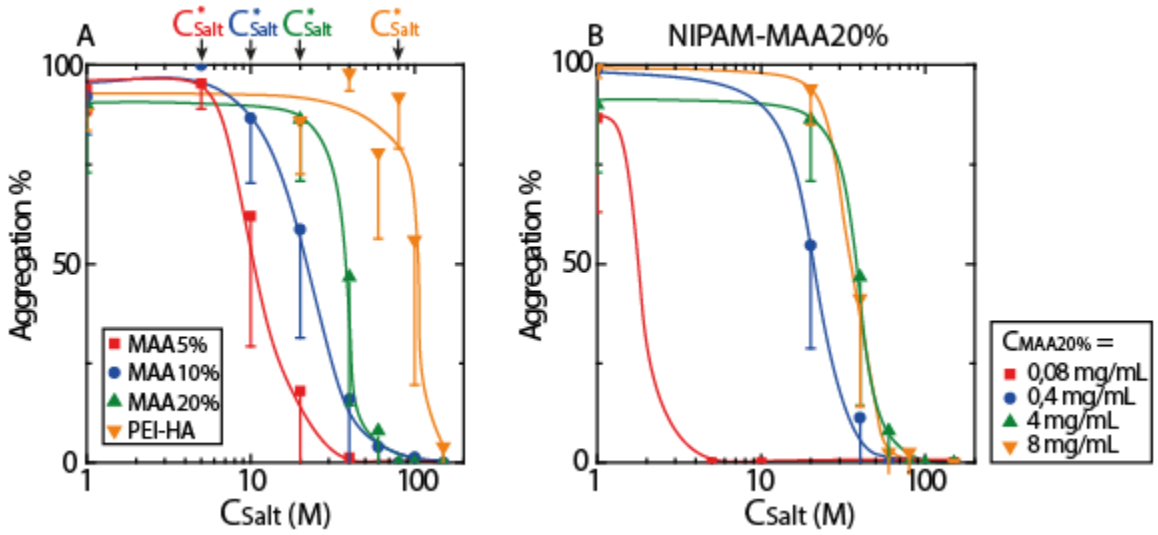

Figure 3-5: Effect of salt concentration on the directed assembly of A) PEI/HA and PEI/MG systems B) PEI/MG system in presence of microgels NIPAM-MAA20% at different concentrations. Lines are guides for the eye.

Since the two systems under study are composed of pH-sensitive materials, the effect of pH on the directed assembly of the hydrogel blocks was also studied. We compared our previous

results obtained in pure water (pH = 6) with tests performed in acidic (pH = 3) and basic (pH = 10.5) conditions (see Figure6). Results show a complete loss of assembly at a pH above or below pH = 6 after 24h of equilibrium.

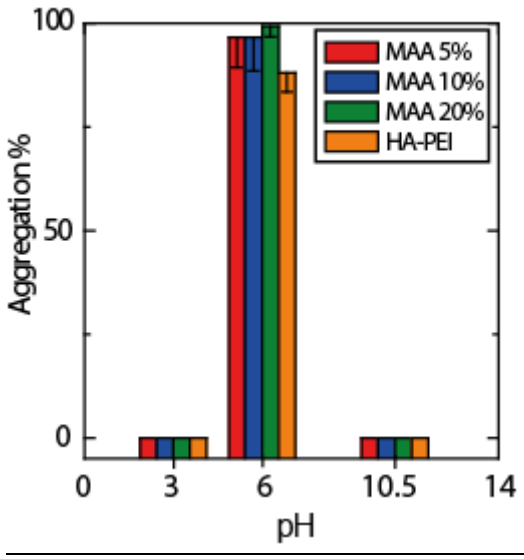

Figure 3-6: Effect of pH on the directed assembly of PEI/HA and PEI/MG systems

Discussion

Simple macroscopic observations of the blocks aggregates pointed out differences in interaction strength between PEI/HA and PEI/MG systems. Larger and more flexible PEI/HA aggregates were indeed systematically observed compared to more compact and rigid PEI/MG aggregates.

For the PEI/HA system, we observed that the blocks concentration (population size) played an important role in determining the aggregates size, which means that every random contact between positive and negative blocks did not necessarily lead to an adhesive contact. Nevertheless, only adhesive contacts between positive and negative blocks were observed, demonstrating that directed assembly, in opposition to self-assembly, was effectively happening. The total loss of assembly capacity of the PEI/HA blocks after a few iterations strongly suggest that the hydrogel blocks surfaces are very sensitive to mechanical manipulation

and therefore prone to damage. Surface damage can occur in the form of surface roughening or material transfer between surfaces (which leads to surface charge compensation), both causes leading to adhesion loss and consequently to a decrease of the aggregation number. Those initials observations suggested that in the case of the PEI/HA system, adhesive contacts are mostly promoted by steric entanglements and electrostatic interactions between polyelectrolytes chains present at the hydrogel blocks surfaces (See Figure 7A).

We observed that the effect of C_{Salt} on the blocks aggregation is not gradual, meaning that the aggregates size did not continuously decrease with salt concentration. Instead, an abrupt transition from an aggregated to a disaggregated state was observed around C^*_{Salt}. Surprisingly, C^*_{Salt} was found to be much higher for HA/PEI system suggesting that other than purely electrostatic forces might be at work in this system. In fact, the poor reproducibility of the assembly process for HA-PEI blocks and the high C^*_{Salt} value indicate that electrostatic and macromolecular entanglements are involved in the adhesion mechanism.

Since HA and PEI are polyelectrolytes, their ionization degree is directly determined by the pH of the medium. HA possess carboxylic acid groups with a pKa around 3-4[36]. While HA chains are only partially negatively charged at pH=3 (24% ionization, pH ≈ pKa), at pH = 6 and 10 HA is fully neutralized (pH >pKa). On the other hand, branched PEI possess primary, secondary and tertiary amines and therefore three respective pKa (4.5, 6.7 and 11.6 [37]). Using the structure of the branched PEI used in this study (primary:secondary:tertiary amines ratio of 4:3:4), the total amount of ionized amine groups (in form of NH^+, NH_2^+ and NH_3^+) available on the polyelectrolyte chains at a given pH can be estimated. At pH = 3, 98.9% of amine groups are positively charged, 60.2% at pH =6 (secondary and tertiary amines) and only 33.7% at pH = 10.5 (tertiary amines only). To insure adhesive electrostatic interactions between blocks surfaces, negative and positive surfaces must be highly ionized. This explained why assembly was only observed at pH

=6. At pH = 6, blocks exposed enough charged groups (99.7% for HA and 60.2% for PEI), which was not the case at pH =3 (24% HA ionization) and 10. (33.7% PEI ionization). Moreover, ionization can also have an effect on polyelectrolyte chains conformation. At high ionization degree, polymer chains from one block surface are expected to expand which favors overlapping and entanglement upon contact with another surface. Therefore, our study shows that assembly of hydrogel blocks can occur at partial ionization of the polyelectrolytes (60% for PEI) but can be inhibited if ionization is too small (the minimum being located between 30 and 60%).

As for the PEI/MG systems, MGs were found to act as efficient adhesion promoters between positively charged blocks. By electrostatically interacting with the PEI chains and potentially the network of HEMA-PEGDMA forming the blocks, MGs can form a negatively charged layer at the block surfaces which promotes electrostatic bridging with bare PEI chains (See Figure 7B).

Since the MGs are significantly more crosslinked than the hydrogel blocks, interpenetration between polyelectrolytes chains and MGs is expected to be disfavored. Therefore, microgel adsorption and blocks adhesion are both driven by MAA groups at the surface of the microgel.

This explanation is also confirmed by the fact that no directed assembly with MGs of pure NIPAM (which were found to be slightly charged) was observed.

The fact that we have not observed any self-aggregation between PEI blocks during the microgel pretreatments of the blocks, even at low MG concentration, demonstrates that adhesion is only possible between treated and non-treated blocks. This can be explained either by the presence of a repulsive electrostatic force between microgel layers on the blocks surfaces or either by an increase in roughness of the blocks surfaces[38].

One major difference compared to the PEI/HA system is the surprisingly good directed assembly reproducibility after several iterations (See Figure 3), indicating that the blocks surfaces were

not damaged under mechanical manipulation, and that PEI/MG interactions are perfectly reversible.

The effect of the ionic strength seems to be modulated by the composition of the microgels. C^*_{Salt} was found to increase strongly with MAA% in the microgels from 5mM for MAA5% to 20mM for MAA20%. This confirms the crucial role of MAA on the interactions at block surfaces. The disrupting effect of NaCl is explained by the hindering of the interactions between MAA at microgel surfaces and PEI chains and the microgel size variation (See Figure 5A). Higher MAA% and larger microgels could also explain the increased C^*_{Salt} as more chloride anions are needed to completely screen PEI-microgels interactions. Stability tests also confirmed that microgels are stable at very high C_{Salt} (data not shown). The salt critical coagulation concentrations of the microgels are indeed significantly higher than the C_{Salt} used in our tests meaning that the microgels remain stable and, at least in part, electrostatically charged and thus prone to interactions with PEI chains. Loss of directed assembly could also be due to PEI polyelectrolytes chains reorganization and folding, decreasing possible interactions with microgels.

The influence of pH on the directed assembly of PEI/MG is quite similar to PEI/HA system. Linear MAA chains with a degree of polymerization superior to20, present a pKa of 6.5[39]. Considering this information, microgels should exhibit no ionization of the MAA at pH=3 and complete ionization at pH=10.5 (>99.9%). Therefore, in acidic or basic conditions, MAA and PEI are not ionized enough to obtain electrostatic interactions. At pH=6, MAA presents 24.0% of ionization which seems sufficient to promote interactions with the charged amines of the PEI. However, the fate of the microgels after PEI/MG block equilibrations at pH=3 and 10.5 solutions remains unknown. It is indeed unclear if microgels stay adsorbed or entrapped in the HEMA-PEDGMA and PEI networks or if they were released upon loss of ionization.

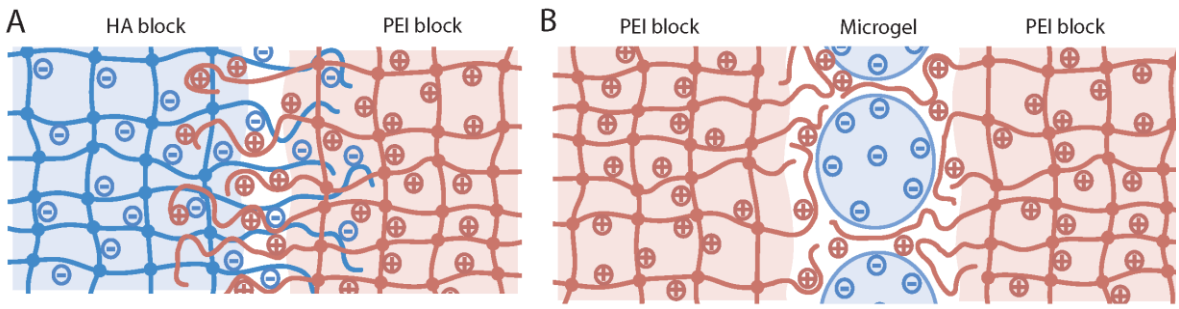

Figure 3-7: Models of supposed interactions at hydrogel blocks surfaces during adhesive contacts, A: steric entanglement guided by electrostatic cues between HA and PEI polyelectrolytes chains, B: bridging between PEI chains and NIPAM-MAA microgels without any entanglements involved.

In summary, the assembly of PEI/HA blocks were found to be driven by electrostatic interactions and steric entanglements. As a consequence, this system was prone to surface damage by mechanical manipulation. The PEI/MG system is based on the reversible electrostatic interactions between ionized MAA groups in the MGs and PEI polyelectrolytes chains. This systems was not damaged under mechanical manipulation but was highly sensitive to ionic strength. These observations highlight the role of the interface microstructure in the adhesion mechanism (see Figure 7). Hydrogel-hydrogel interfaces in presence of microgels are expected to be rougher compared to direct hydrogel-hydrogel contacts allowing for ions to quickly penetrate the interface and to destabilize it even if the adhesive strength between blocks is stronger.

Conclusion

This study presents the directed assembly of charged hydrogel blocks mediated by microgel particles or by direct contact. In both systems studied, direct contact between PEI/HA blocks or between MGs and PEI blocks, random contacts between blocks resulted in the formation of aggregates. PEI/HA directed assembly in water resulted in large, flexible and vulnerable to

mechanical manipulation aggregates while PEI/MG aggregates were more compact and resistant. Such difference was attributed to a difference in adhesion strength between blocks. The PEI/MG system presented the highest sensitivity to ionic strength, highlighting the role of the interface microstructure and porosity in the adhesion phenomena.

These results provide new insights into the adhesion mechanism between soft materials in presence of a third body such as microgels, proteins or solid nanoparticles and should guide the development of future materials with controlled tunable properties.

Acknowledgements

XB is grateful for the financial support of FRQ-NT (new researcher program) and CRC. NH acknowledges the financial support of the Faculty of Pharmacy (recruitment scholarship). PLL is grateful for financial support of GRUM, Faculty of Pharmacy, FRQ-NT and NSERC.

References

1. Hoffman, A. S. Hydrogels for biomedical applications. *Adv. Drug Del. Rev.* **2012,***64, Supplement*, 18-23.
2. King, W. J.; Krebsbach, P. H. Growth factor delivery: How surface interactions modulate release in vitro and in vivo. *Adv. Drug Del. Rev.* **2012,***64* (12), 1239-1256.
3. Hanauer, N.; Latreille, P.; Alsharif, S.; Banquy, X. 2D, 3D and 4D Active Compound Delivery in Tissue Engineering and Regenerative Medicine. *Curr. Pharm. Des.* **2015**.
4. Hoare, T. R.; Kohane, D. S. Hydrogels in drug delivery: progress and challenges. *Polymer* **2008,***49* (8), 1993-2007.
5. Priya, S. G.; Jungvid, H.; Kumar, A. Skin tissue engineering for tissue repair and regeneration. *Tissue Eng. Pt B-Rev* **2008,***14* (1), 105-118.
6. Metcalfe, A. D.; Ferguson, M. W. J. Bioengineering skin using mechanisms of regeneration and repair. *Biomaterials* **2007,***28* (34), 5100-5113.
7. Lam, J.; Clark, E. C.; Fong, E. L. S.; Lee, E. J.; Lu, S.; Tabata, Y.; Mikos, A. G. Evaluation of cell-laden polyelectrolyte hydrogels incorporating poly(l-Lysine) for applications in cartilage tissue engineering. *Biomaterials* **2016,***83*, 332-346.
8. Muzzarelli, R. A. A.; Greco, F.; Busilacchi, A.; Sollazzo, V.; Gigante, A. Chitosan, hyaluronan and chondroitin sulfate in tissue engineering for cartilage regeneration: A review. *Carbohydrate Polymers* **2012,***89* (3), 723-739.
9. Griffin, K. S.; Davis, K. M.; McKinley, T. O.; Anglen, J. O.; Chu, T.-M. G.; Boerckel, J. D.; Kacena, M. A. Evolution of Bone Grafting: Bone Grafts and Tissue Engineering Strategies for Vascularized Bone Regeneration. *Clin. Rev. Bone. Miner. Metab.* **2015,***13* (4), 232-244.
10. Yang, J.-A.; Yeom, J.; Hwang, B. W.; Hoffman, A. S.; Hahn, S. K. In situ-forming injectable hydrogels for regenerative medicine. *Prog. Polym. Sci.* **2014,***39* (12), 1973-1986.
11. Shu, X. Z.; Liu, Y.; Palumbo, F. S.; Luo, Y.; Prestwich, G. D. In situ crosslinkable hyaluronan hydrogels for tissue engineering. *Biomaterials* **2004,***25* (7), 1339-1348.
12. Cai, S.; Liu, Y.; Shu, X. Z.; Prestwich, G. D. Injectable glycosaminoglycan hydrogels for controlled release of human basic fibroblast growth factor. *Biomaterials* **2005,***26* (30), 6054-6067.
13. Tsukuda, Y.; Onodera, T.; Ito, M.; Izumisawa, Y.; Kasahara, Y.; Igarashi, T.; Ohzawa, N.; Todoh, M.; Tadano, S.; Iwasaki, N. Therapeutic effects of intra-articular ultra-purified low endotoxin alginate administration on an experimental canine osteoarthritis model. *Journal of Biomedical Materials Research Part A* **2015,***103* (11), 3441-3448.
14. Kim, G. O.; Kim, N.; Kim, D. Y.; Kwon, J. S.; Min, B.-H. An electrostatically crosslinked chitosan hydrogel as a drug carrier. *Molecules* **2012,***17* (12), 13704-13711.
15. Salem, A. K.; Rose, F. R.; Oreffo, R. O.; Yang, X.; Davies, M. C.; Mitchell, J. R.; Roberts, C. J.; Stolnik-Trenkic, S.; Tendler, S. J.; Williams, P. M. Porous polymer and cell composites that self-assemble in situ. *Adv. Mater.* **2003,***15* (3), 210-213.
16. Miyata, T.; Asami, N.; Uragami, T. Preparation of an antigen-sensitive hydrogel using antigen-antibody bindings. *Macromolecules* **1999,***32* (6), 2082-2084.
17. Sant, S.; Coutinho, D. F.; Sadr, N.; Reis, R. L.; Khademhosseini, A. Tissue Analogs by the Assembly of Engineered Hydrogel Blocks. *Biomimetic Approaches for Biomaterials Development* **2012**, 471-493.
18. Whitesides, G. M.; Boncheva, M. Beyond molecules: Self-assembly of mesoscopic and macroscopic components. *Proceedings of the National Academy of Sciences* **2002,***99* (8), 4769-4774.

19. Cheng, H.-w.; Luk, K. D. K.; Cheung, K. M. C.; Chan, B. P. In vitro generation of an osteochondral interface from mesenchymal stem cell–collagen microspheres. *Biomaterials* **2011,***32* (6), 1526-1535.
20. Tan, W.; Desai, T. A. Layer-by-layer microfluidics for biomimetic three-dimensional structures. *Biomaterials* **2004,***25* (7–8), 1355-1364.
21. McGuigan, A. P.; Sefton, M. V. Vascularized organoid engineered by modular assembly enables blood perfusion. *Proceedings of the National Academy of Sciences* **2006,***103* (31), 11461-11466.
22. Chung, S. E.; Park, W.; Shin, S.; Lee, S. A.; Kwon, S. Guided and fluidic self-assembly of microstructures using railed microfluidic channels. *Nature materials* **2008,***7* (7), 581-587.
23. Du, Y.; Lo, E.; Ali, S.; Khademhosseini, A. Directed assembly of cell-laden microgels for fabrication of 3D tissue constructs. *Proceedings of the National Academy of Sciences of the United States of America* **2008,***105* (28), 9522-9527.
24. Fernandez, J. G.; Khademhosseini, A. Micro-masonry: construction of 3D structures by microscale self-assembly. *Adv. Mater.* **2010,***22* (23), 2538-2541.
25. Xu, M.; Wang, X.; Yan, Y.; Yao, R.; Ge, Y. An cell-assembly derived physiological 3D model of the metabolic syndrome, based on adipose-derived stromal cells and a gelatin/alginate/fibrinogen matrix. *Biomaterials* **2010,***31* (14), 3868-3877.
26. Ekici, S.; Ilgin, P.; Yilmaz, S.; Aktas, N.; Sahiner, N. Temperature and magnetic field responsive hyaluronic acid partides with tunable physical and chemical properties. *Appl. Surf. Sci.* **2011,***257* (7), 2669-2676.
27. Liu, B.; Liu, Y.; Lewis, A. K.; Shen, W. Modularly assembled porous cell-laden hydrogels. *Biomaterials* **2010,***31* (18), 4918-4925.
28. Harada, A.; Kobayashi, R.; Takashima, Y.; Hashidzume, A.; Yamaguchi, H. Macroscopic self-assembly through molecular recognition. *Nature chemistry* **2011,***3* (1), 34-37.
29. Yamaguchi, H.; Kobayashi, Y.; Kobayashi, R.; Takashima, Y.; Hashidzume, A.; Harada, A. Photoswitchable gel assembly based on molecular recognition. *Nature communications* **2012,***3*, 603.
30. Qi, H.; Ghodousi, M.; Du, Y.; Grun, C.; Bae, H.; Yin, P.; Khademhosseini, A. DNA-directed self-assembly of shape-controlled hydrogels. *Nature communications* **2013,***4*.
31. Gillette, B. M.; Jensen, J. A.; Tang, B.; Yang, G. J.; Bazargan-Lari, A.; Zhong, M.; Sia, S. K. In situ collagen assembly for integrating microfabricated three-dimensional cell-seeded matrices. *Nature materials* **2008,***7* (8), 636-640.
32. Yu, Y.; Kieviet, B. D.; Kutnyanszky, E.; Vancso, G. J.; de Beer, S. Cosolvency-induced switching of the adhesion between poly (methyl methacrylate) brushes. *ACS macro letters* **2014,***4* (1), 75-79.
33. Cao, Z.; Dobrynin, A. V. Nanoparticles as Adhesives for Soft Polymeric Materials. *Macromolecules* **2016,***49* (9), 3586-3592.
34. Rose, S.; Prevoteau, A.; Elzière, P.; Hourdet, D.; Marcellan, A.; Leibler, L. Nanoparticle solutions as adhesives for gels and biological tissues. *Nature* **2014,***505* (7483), 382-385.
35. Brunel, B.; Beaune, G.; Nagarajan, U.; Dufour, S.; Brochard-Wyart, F.; Winnik, F. M. Nanostickers for cells: a model study using cell–nanoparticle hybrid aggregates. *Soft Matter* **2016,***12* (38), 7902-7907.
36. Mero, A.; Campisi, M. Hyaluronic acid bioconjugates for the delivery of bioactive molecules. *Polymers* **2014,***6* (2), 346-369.
37. Demadis, K. D.; Paspalaki, M.; Theodorou, J. Controlled release of bis (phosphonate) pharmaceuticals from cationic biodegradable polymeric matrices. *Industrial & Engineering Chemistry Research* **2011,***50* (9), 5873-5876.

38. Fuller, K.; Tabor, D. In *The effect of surface roughness on the adhesion of elastic solids*, Proceedings of the Royal Society of London A: Mathematical, Physical and Engineering Sciences, 1975; The Royal Society, pp 327-342.
39. Izumrudov, V. A.; Kharlampieva, E.; Sukhishvili, S. A. Multilayers of a globular protein and a weak polyacid: role of polyacid ionization in growth and decomposition in salt solutions. *Biomacromolecules* **2005,***6* (3), 1782-1788.

Chapitre 4:Conclusion

Notre objectif était la mise en place d'un système de fabrication simple et réutilisable de blocs hydrogels de taille et forme contrôlées possédant des fonctionnalisations permettant des interactions électrostatiques adhésives résultant en des propriétés d'auto-assemblage. Nous avons ainsi développé un procédé de fabrication se basant sur la photolithographie. L'utilisation de polycations (PEI), de polyanions (HA) et de particules microgels chargées négativement (NIPAM-MAA), nous a permis d'obtenir des blocs chargés positivement et négativement. La mise en contact aléatoire de mélanges de blocs nous a permis de créer des assemblages dirigés pour les deux systèmes étudiés (PEI/HA et PEI/MG). Les deux systèmes présentent cependant des propriétés d'adhésion différentes laissant suggérer des mécanismes adhésifs distincts : les assemblages PEI/HA sont en effet plus flexibles et fragiles que les assemblages PEI/MG plus compacts et résistants. Ces derniers ont montré de plus des propriétés adhésives modulables avec la taille et le pourcentage en MAA des particules microgels utilisés. Une autre différence des comportements adhésifs s'est manifestée dans les milieux salins puisque les systèmes PEI/MG possèdent des concentrations limites salines permettant l'agrégation beaucoup plus faible que le système PEI/HA. Enfin, les deux systèmes n'ont démontré aucune propriété d'assemblage dirigé en milieu acide ou basique. Nous pensons d'une part que le système PEI/HA se base sur un mélange d'interactions stériques et électrostatiques entre polyélectrolytesde charges opposées et d'autre part que le système PEI/MG se base sur des interactions purement électrostatiques focalisés sur les microgels.

Chapitre 5 : Perspectives et travaux futurs

Les travaux présentés dans ce mémoire ouvrent la voie à de nombreuses perspectives et différents axes de recherche sont envisageables et complémentaires.

L'utilisation d'autres fonctionnalisations, impliquant un plus grand choix d'interactions adhésives possibles, serait intéressante car elle pourrait entrainer un meilleur contrôle sur l'auto-assemblage des échafaudages pouvant résulter en des structures plus complexes. Outre l'utilisation d'autres polyélectrolytes et microgels, le mélange avec d'autres types de fonctionnalisations adhésives (interactions ligand-récepteur, branches complémentaires d'ADN, groupes chimiques réactifs) est envisageable. Cet effort de complexification pourra aussi prendre la forme d'utilisation de formes de blocs différentes et le développement de fonctionnalisation sur des surfaces spécifiques par utilisation de techniques comme la microfluidique.

Une meilleure compréhension des mécanismes adhésifs permettrait une meilleure utilisation de ceux-ci. Il serait ainsi intéressant d'aller observer les propriétés de nos surfaces (rugosité, porosité, propriétés électrostatiques) et les interactions adhésives développées au niveau moléculaire. Pour cela, l'expertise et l'équipement du Pr. Banquy et du Laboratoire de caractérisation des matériaux de nos confrères de la faculté de chimie seront un atout majeur. Il serait ainsi possible d'examiner les fonctionnalisations de nos surfaces et les interactions adhésives résultantes avec l'utilisation de l'appareil à force de surface (SFA) de notre laboratoire ainsi que les techniques de microscopies à force atomique, à force électrique et Kelvin Probe.

Un effort devra être porté sur l'amélioration des techniques de synthèse des blocs hydrogels. Le développement de solutions thérapeutiques se basant sur l'auto-assemblage d'échafaudages hydrogel nécessitera en effet l'obtention de blocs de taille permettant l'injection. L'utilisation de masques de meilleures qualités et plus précis ainsi qu'une meilleure gestion de l'application à la lumière UV permettra d'obtenir des blocs microscopiques.

Enfin il sera crucial d'investiguer le potentiel des échafaudages auto-assemblés pour le support et la croissance de cultures cellulaires. Il est premièrement envisagé dans notre étudie d'utiliser des chondrocytes à la base du développement des tissus cartilagineux. Dans un premier temps, des études pourront être menées pour caractériser la croissance cellulaire à l'intérieur des blocs mais aussi à l'interface entre blocs, ou les propriétés physico-chimiques peuvent varier par rapport au cœur de notre matériau hydrogel. Dans un deuxième temps, il faudra développer des preuves de concept sur le possible contrôle de la croissance tissulaire à l'aide des possibilités d'assemblage dirigé et de relargage de facteurs de croissance depuis certains blocs.

Références

1. Badylak, S. and N. Rosenthal, *Regenerative medicine: are we there yet?* npj Regenerative Medicine, 2017. **2**(1): p. 2.
2. Wobma, H. and G. Vunjak-Novakovic, *Tissue engineering and regenerative medicine 2015: a year in review.* Tissue Engineering Part B: Reviews, 2016. **22**(2): p. 101-113.
3. Barrilleaux, B., et al., *Review: ex vivo engineering of living tissues with adult stem cells.* Tissue engineering, 2006. **12**(11): p. 3007-3019.
4. Martinod, E., et al., *In Vivo Tissue Engineering of Human Airways.* The Annals of Thoracic Surgery, 2017.
5. Shanbhag, S., et al., *Bone tissue engineering in oral peri-implant defects in preclinical in vivo research: a systematic review and meta-analysis.* Journal of Tissue Engineering and Regenerative Medicine, 2017.
6. Dhaliwal, K., R. Kunchur, and R. Farhadieh, *Review of the cellular and biological principles of distraction osteogenesis: An in vivo bioreactor tissue engineering model.* Journal of Plastic, Reconstructive & Aesthetic Surgery, 2016. **69**(2): p. e19-e26.
7. Tonelli, F.M.P., et al., *Stem Cells and Tissue Engineering*, in *Working with Stem Cells*. 2016, Springer. p. 331-346.
8. Caplan, A.I., *Adult mesenchymal stem cells for tissue engineering versus regenerative medicine.* Journal of cellular physiology, 2007. **213**(2): p. 341-347.
9. Tuan, R.S., G. Boland, and R. Tuli, *Adult mesenchymal stem cells and cell-based tissue engineering.* Arthritis Research & Therapy, 2003. **5**(1): p. 32-45.
10. Lutolf, M. and J. Hubbell, *Synthetic biomaterials as instructive extracellular microenvironments for morphogenesis in tissue engineering.* Nature biotechnology, 2005. **23**(1): p. 47-55.
11. Place, E.S., N.D. Evans, and M.M. Stevens, *Complexity in biomaterials for tissue engineering.* Nat Mater, 2009. **8**(6): p. 457-470.
12. Li, Y., Y. Xiao, and C. Liu, *The Horizon of Materiobiology: A Perspective on Material-Guided Cell Behaviors and Tissue Engineering.* Chemical reviews, 2017.
13. Green, J.J. and J.H. Elisseeff, *Mimicking biological functionality with polymers for biomedical applications.* Nature, 2016. **540**(7633): p. 386-394.
14. Slaughter, B.V., et al., *Hydrogels in Regenerative Medicine.* Advanced Materials, 2009. **21**(32-33): p. 3307-3329.
15. Priya, S.G., H. Jungvid, and A. Kumar, *Skin tissue engineering for tissue repair and regeneration.* Tissue Engineering Part B: Reviews, 2008. **14**(1): p. 105-118.
16. Metcalfe, A.D. and M.W. Ferguson, *Bioengineering skin using mechanisms of regeneration and repair.* Biomaterials, 2007. **28**(34): p. 5100-5113.
17. Lam, J., et al., *Evaluation of cell-laden polyelectrolyte hydrogels incorporating poly (l-Lysine) for applications in cartilage tissue engineering.* Biomaterials, 2016. **83**: p. 332-346.
18. Muzzarelli, R.A., et al., *Chitosan, hyaluronan and chondroitin sulfate in tissue engineering for cartilage regeneration: A review.* Carbohydrate Polymers, 2012. **89**(3): p. 723-739.
19. Griffin, K.S., et al., *Evolution of bone grafting: bone grafts and tissue engineering strategies for vascularized bone regeneration.* Clinical Reviews in Bone and Mineral Metabolism, 2015. **13**(4): p. 232-244.

20. Khademhosseini, A. and R. Langer, *Microengineered hydrogels for tissue engineering.* Biomaterials, 2007. **28**(34): p. 5087-5092.
21. Kondiah, P.J., et al., *A Review of Injectable Polymeric Hydrogel Systems for Application in Bone Tissue Engineering*. Molecules, 2016. **21**(11): p. 1580.
22. Vo, T.N., et al., *Acellular mineral deposition within injectable, dual-gelling hydrogels for bone tissue engineering.* Journal of Biomedical Materials Research Part A, 2017. **105**(1): p. 110-117.
23. Sant, S., et al., *Tissue Analogs by the Assembly of Engineered Hydrogel Blocks.* Biomimetic Approaches for Biomaterials Development, 2012: p. 471-493.
24. Whitesides, G.M. and M. Boncheva, *Beyond molecules: Self-assembly of mesoscopic and macroscopic components.* Proceedings of the National Academy of Sciences, 2002. **99**(8): p. 4769-4774.
25. Cheng, H.-w., et al., *In vitro generation of an osteochondral interface from mesenchymal stem cell–collagen microspheres.* Biomaterials, 2011. **32**(6): p. 1526-1535.
26. Tan, W. and T.A. Desai, *Layer-by-layer microfluidics for biomimetic three-dimensional structures.* Biomaterials, 2004. **25**(7): p. 1355-1364.
27. McGuigan, A.P. and M.V. Sefton, *Vascularized organoid engineered by modular assembly enables blood perfusion.* Proceedings of the National Academy of Sciences, 2006. **103**(31): p. 11461-11466.
28. Chung, S.E., et al., *Guided and fluidic self-assembly of microstructures using railed microfluidic channels.* Nature materials, 2008. **7**(7): p. 581-587.
29. Du, Y., et al., *Directed assembly of cell-laden microgels for fabrication of 3D tissue constructs.* Proceedings of the National Academy of Sciences of the United States of America, 2008. **105**(28): p. 9522-9527.
30. Fernandez, J.G. and A. Khademhosseini, *Micro-masonry: construction of 3D structures by microscale self-assembly.* Advanced Materials, 2010. **22**(23): p. 2538-2541.
31. Xu, M., et al., *An cell-assembly derived physiological 3D model of the metabolic syndrome, based on adipose-derived stromal cells and a gelatin/alginate/fibrinogen matrix.* Biomaterials, 2010. **31**(14): p. 3868-3877.
32. Liu, B., et al., *Modularly assembled porous cell-laden hydrogels.* Biomaterials, 2010. **31**(18): p. 4918-4925.
33. Harada, A., et al., *Macroscopic self-assembly through molecular recognition.* Nature chemistry, 2011. **3**(1): p. 34-37.
34. Yamaguchi, H., et al., *Photoswitchable gel assembly based on molecular recognition.* Nature communications, 2012. **3**: p. 603.
35. Qi, H., et al., *DNA-directed self-assembly of shape-controlled hydrogels.* Nature communications, 2013. **4**.
36. Gillette, B.M., et al., *In situ collagen assembly for integrating microfabricated three-dimensional cell-seeded matrices.* Nature materials, 2008. **7**(8): p. 636-640.
37. Yu, Y., et al., *Cosolvency-induced switching of the adhesion between poly (methyl methacrylate) brushes.* ACS macro letters, 2014. **4**(1): p. 75-79.
38. Cao, Z. and A.V. Dobrynin, *Nanoparticles as Adhesives for Soft Polymeric Materials.* Macromolecules, 2016. **49**(9): p. 3586-3592.
39. Rose, S., et al., *Nanoparticle solutions as adhesives for gels and biological tissues.* Nature, 2014. **505**(7483): p. 382-385.
40. Brunel, B., et al., *Nanostickers for cells: a model study using cell–nanoparticle hybrid aggregates.* Soft Matter, 2016. **12**(38): p. 7902-7907.

41. Hoffman, A.S., *Hydrogels for biomedical applications.* Advanced drug delivery reviews, 2012. **64**: p. 18-23.